CHAPTER IV

RESULTS AND DISCUSSION

4.1 Parameter studies and their significance

Styrene-divinylbenzene copolymers were used in the absorption of toluene and some results were presented in Table 4.1. The results were used for multiple variable linear regression. Analysis of variance (ANOVA) was used to show the relation between swelling ratio with respect to each parameter. The independent parameters, x, are the concentrations of toluene, styrene, divinylbenzene, and PVA; while the dependent parameter interested, y_1, is the swelling ratio.

Table 4.1 Dependence of Swelling Ratio on PVA, DVB, Tol(%).

%PVA	%Sty	%DVB	%Tol	Swelling Ratio
0.06	92.5	7.5	100	4.1
0.06	92.5	7.5	100	3.6
0.06	92.5	7.5	100	3.8
0.09	92.5	7.5	100	6.1
0.09	92.5	7.5	100	7.3
0.09	92.5	7.5	100	7.0
0.12	92.5	7.5	100	5.2
0.12	92.5	7.5	100	6.0
0.12	95.0	5.0	100	6.2
0.12	95.0	5.0	100	7.1
0.12	95.0	5.0	100	5.9
0.12	92.5	7.5	100	5.5
0.12	92.5	7.5	100	5.3
0.12	90.0	10	100	4.5
0.12	90.0	10	100	4.2
0.12	90.0	10	100	3.9
0.12	92.5	7.5	30	2.4
0.12	92.5	7.5	60	2.7
0.12	92.5	7.5	60	3.1
0.12	92.5	7.5	100	5.3
0.12	92.5	7.5	100	5.7

[a] BPO 0.5%, 70°C, 240 rpm.

Table 4.2 Summary of the multiple regression equation by ANOVA.

Method	Appropriate equation
1. Forward	$y_1 = 3.681+4.97 \times 10^{-2}$ Tol-0.44 DVB
2. Backward	$y_1 = -40.319+0.44$ Sty$+4.97 \times 10^{-2}$ Tol
3. Stepwise	$y_1 = 3.681+4.97 \times 10^{-2}$ Tol-0.44 DVB

A statistical test about the coefficients of partial correlation of parameter [25]

(H_0): $\rho_{y,xi} \leq 0$ VS (H_1): $\rho_{y,xi} > 0$; $i = 1,2,3,4$

Rejection region: For a given value of $\alpha = 0.05$

Reject H_0 if sig. $< \alpha$

Significance of swelling ratio with independent parameter is 0.377(PVA), 0.029(Sty), 0.029(DVB) and 0.001(Tol). Because the values of significance are less than probability F that styrene, divinylbenzene and toluene are related with swelling ratio. The three methods of ANOVA analysis show the solution that the swelling ratio depends on the amounts of toluene, styrene and divinylbenzene, not that of poly(vinyl alcohol). We anticipated that poly(vinyl alcohol) is a suspending agent which prevents the monomer droplets from coalescing in the aqueous phase. Therefore, poly(vinyl alcohol) concentration should not directly related with swelling ratio.

Consequently, the influences of toluene and DVB on the swelling ratio of the beads are elucidated as follows.

4.2 Kinetics study of the styrene-divinylbenzene copolymer

The kinetic studies of synthesis of styrene-divinylbenzene copolymer beads were prepared by suspension polymerization using PVA as suspending agent and toluene as diluent. Polymeric mixture was sampling at various times of 30, 60, 90, 120, 150, 180 and 240 min. during polymerization. The condition for copolymerization was shown in Table 3.1. Each parameter was studied in the following section.

4.2.1 The effect of the initiator concentration

The effect of the initiator concentration was studied using the standard recipe shown in Table 3.1. Four runs (A, B, C, and D) with duplication were carried out

Table 4.3 Effect of the Initiator Concentration on Kinetics of Copolymerization of Styrene and Divinylbenzene.

Sample[a]	Time (min)	Conversion of individual monomer (%)			Overall conversion (%)	Morphology	Swelling Ratio	SEM in Figure
		Sty	DVB	EVB				
A	0	0	0	0	-	-		
(BPO 0.1%)	30	44.14	60.83	72.65	-	-	-	-
	60	56.69	66.39	75.95	-	-	-	-
	90	64.83	71.37	78.64	-	-	-	-
	120	69.09	73.51	80.15	-	-	-	-
	150	73.84	77.70	83.26	-	-	-	-
	180	84.72	88.26	91.08	5.5	fusion	-	-
	240	87.12	90.22	92.36	6.7	fusion	-	-
B	0	0	0	0	-	-		
(BPO 0.5%)	30	76.42	80.61	85.45	-	-	-	-
	60	77.46	82.51	86.27	-	-	-	-
	90	81.38	86.44	88.72	-	-	-	-
	120	88.41	92.27	93.66	5.6	fusion	-	-
	150	92.25	95.26	96.00	9.8	fusion	-	-
	180	92.69	95.18	95.70	14.3	coalescence	5.0	-
	240	94.57	96.87	96.88	18.9	coalescence	14.4	4.1
C	0	0	0	0	-	-		
(BPO 1.5%)	30	80.36	84.98	88.01	-	-	-	-
	60	83.19	87.91	89.64	-	-	-	-
	90	88.77	92.60	93.40	-	-	-	-
	120	94.42	97.09	97.23	11.4	fusion	-	-
	150	94.67	97.06	96.94	17.1	coalescence	9.5	-
	180	94.77	97.38	97.07	19.9	coalescence	6.6	-
	240	94.96	97.81	97.17	26.3	coalescence	15.3	4.1
D	0	0	0	0	-	-		
(BPO 2.0%)	30	81.03	85.92	88.68	-	-	-	-
	60	84.29	88.97	90.33	-	-	-	-
	90	89.34	93.21	93.81	-	-	-	-
	120	95.46	97.92	97.91	14.9	fusion	-	-
	150	96.14	98.07	97.91	21.9	coalescence	6.8	-
	180	96.92	100.00	98.34	23.0	coalescence	9.2	-
	240	97.74	100.00	98.98	31.2	coalescence	7.5	4.1

[a] Sty 92.5%, DVB 7.5%, 70°C, 240 rpm., Tol 100%, PVA 0.09%, Monomer: H_2O, 1:7

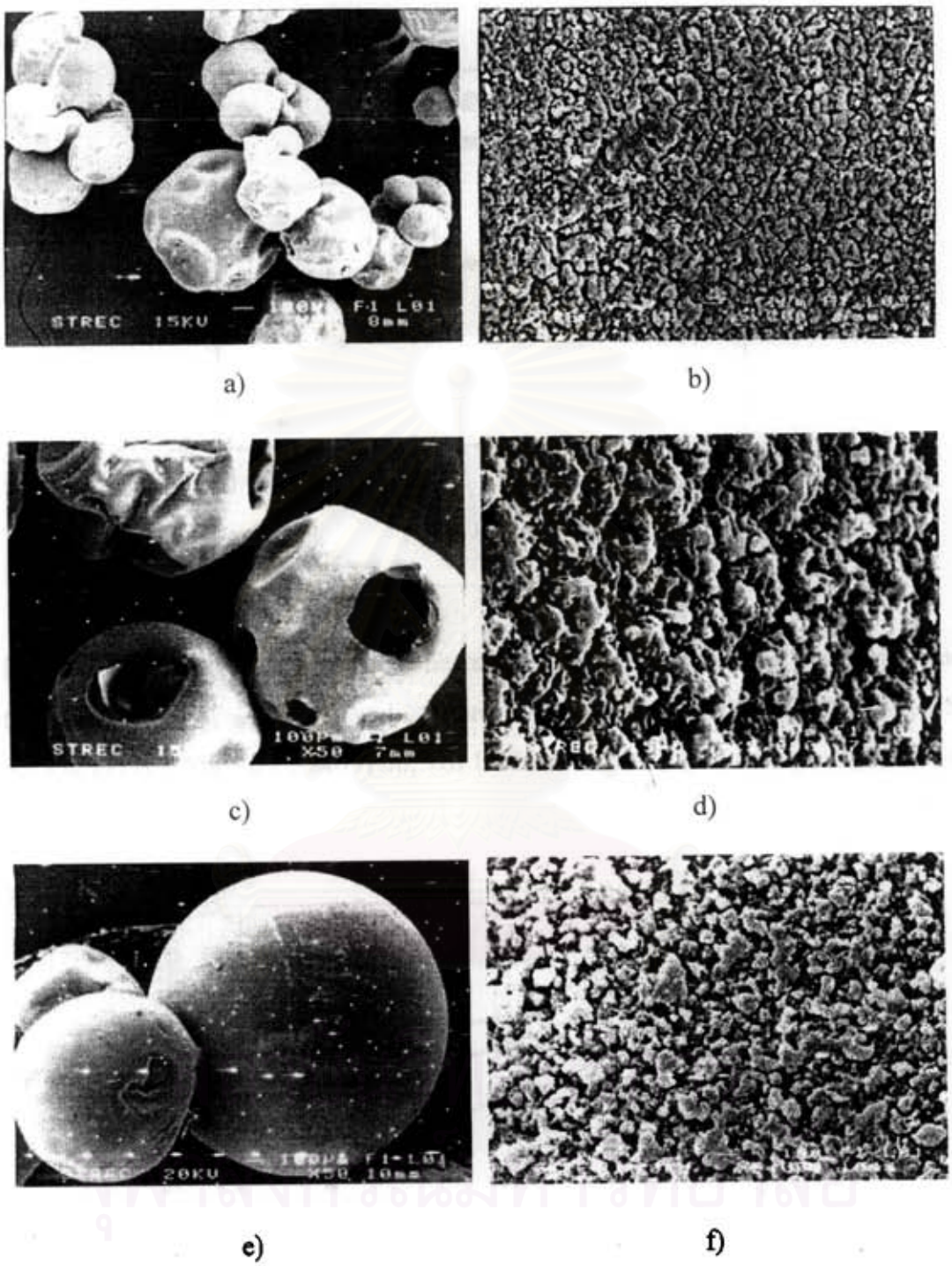

Figure 4.1. Scanning Electron Micrographs of the beads under the effect of the initiator concentration : Sty 92.5%, DVB 7.5%, 70°C, 240 rpm., Tol 100%, PVA 0.09%, Monomer: H_2O, 1:7 at 240 min. of the reaction time.

a) Sample B: BPO 0.5% (x 50) b) Sample B: BPO 0.5% (x 5000)

c) Sample C: BPO 1.5% (x 50) d) Sample C: BPO 1.5% (x 5000)

e) Sample D: BPO 2.0% (x 50) f) Sample D: BPO 2.0% (x 5000)

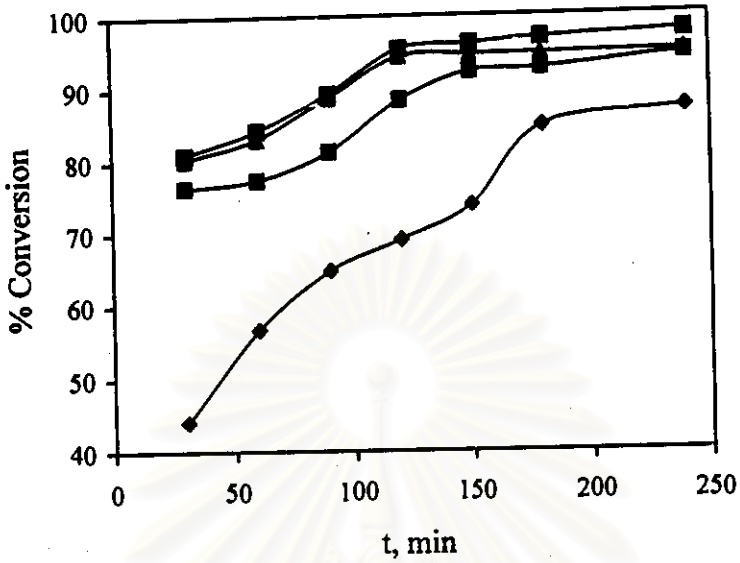

Figure 4.2 Effect of the initiator concentration on conversion of styrene monomer; (The curves ♦♦♦, ■■■, ▲▲▲, and ××× are for BPO 0.1, 0.5, 1.5, and 2.0%; when Sty 92.5%, DVB 7.5%, 70°C, 240 rpm., Tol 100%, PVA 0.09%, Monomer: H_2O, 1:7; are used).

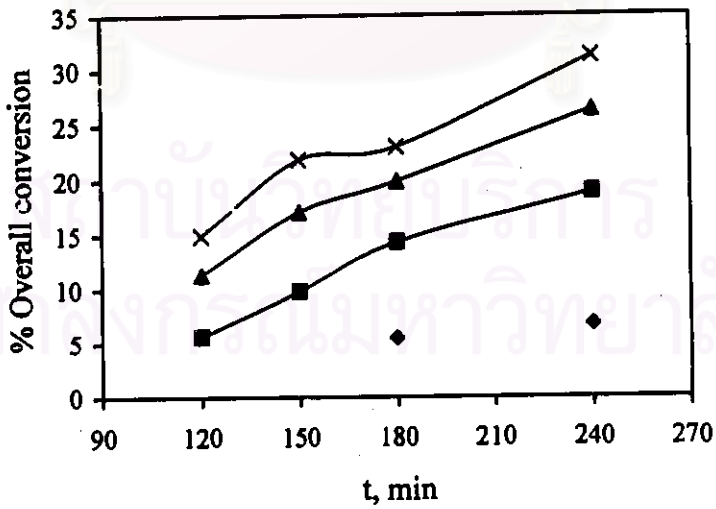

Figure 4.3 Effect of the initiator concentration on overall conversion of styrene-divinylbenzene; (The curves ♦♦♦, ■■■, ▲▲▲, and ××× are for BPO 0.1, 0.5, 1.5, and 2.0%; when Sty 92.5%, DVB 7.5%, 70°C, 240 rpm., Tol 100%, PVA 0.09%, Monomer: H_2O, 1:7; are used).

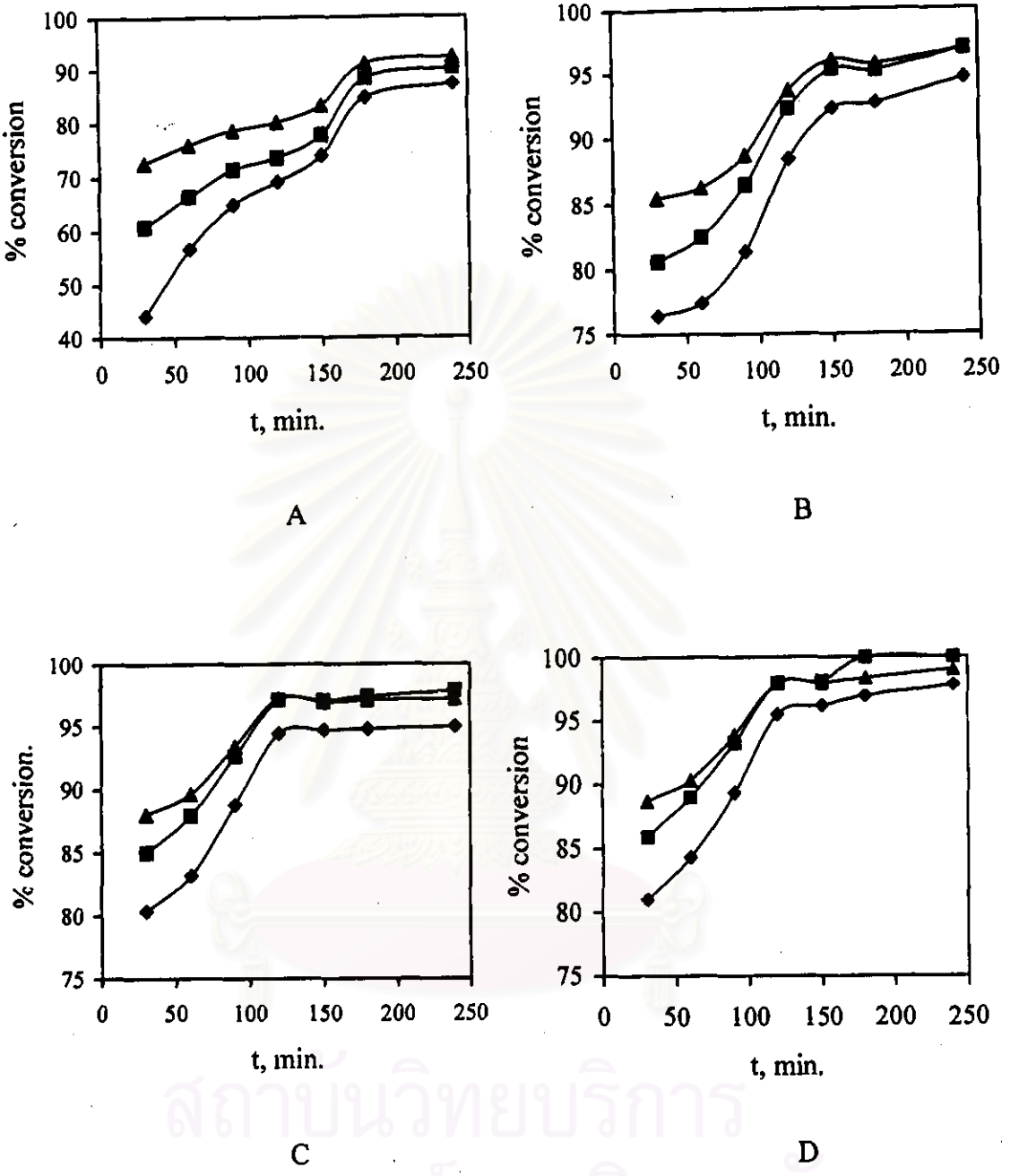

Figure 4.4 Effect of the initiator concentration on conversion of individual monomers (The curves ◆◆◆, ■■■, and ▲▲▲ are for Sty, DVB, and EVB; when Sty 92.5%, DVB 7.5%, Tol 100%, Monomer: H_2O, 1:7, 70°C, 240 rpm., PVA 0.09%, BPO initiator concentration for Sample A (0.1%), Sample B (0.5%), Sample C (1.5%), Sample D (2.0%).

สถาบันวิทยบริการ
จุฬาลงกรณ์มหาวิทยาลัย

using four different concentrations (0.1%, 0.5%, 1.5% and 2.0% based on the monomer phase). The conversion of the individual monomers is followed by gas chromatographic technique which was then shown in Table 4.3 and Figure 4.4. The overall conversion of solid copolymer was determined gravimetrically which was then shown in Table 4.3 and Figure 4.3. The result shows that the conversion increases with the increasing initiator concentration.

Table 4.3, and Figures 4.2, 4.3 and 4.4 show that the initial concentration of the initiator increases from %BPO: 0.1, 0.5, 1.5, and 2.0, respectively; based on monomer phase, the conversion and the overall conversion increases due to more initiator radicals formed in the initiation step.

The more the initiator concentration, the higher the polymer obtain. A conversion curve is shown in Figure 4.2 and overall conversion is shown in Figure 4.3. The conversion curves are shown on Figure 4.4. It is confirmed that DVB is consumed more readily than is styrene. The rate of producing primary radicals by thermal homolysis of an initiator is given by Eq. 2.6. The rate of producing primary radicals is increased when the initiator concentration increases.

At 240 min., (Table 4.3) the polymer formed was clustered and fused to a big lump (no bead formation). Droplet coalescence may occur when two droplets of monomer phase due to their instability in the aqueous phase.

4.2.2 The effect of the temperature

The effect of the temperature was studied using the standard recipe shown in Table 3.1. Three runs (E, B, and F) were carried out using three different temperatures (60, 70, and 80°C). The conversion of the individual monomers was followed by gas chromatographic technique, which was shown in Table 4.4 and Figure 4.9. The overall conversion of polymer was determined gravimetrically which was then shown in Table 4.4 and Figure 4.8. The result shows that the conversion increases when the temperature increases.

Table 4.4 Effect of the Temperature on Kinetics of Copolymerization of Styrene and Divinylbenzene.

Sample[a]	Time (min)	Conversion of individual monomer (%)			Overall conversion (%)	Morphology	Swelling Ratio	SEM in Figure
		Sty	DVB	EVB				
E	0	0	0	0	-	-		
(60°C)	30	70.90	74.95	81.67	-	-	-	-
	60	72.60	81.06	86.46	-	-	-	-
	90	75.43	79.79	84.62	-	-	-	-
	120	75.96	79.70	84.60	-	-	-	-
	150	79.13	82.96	86.77	-	-	-	-
	180	83.50	87.37	90.06	-	-	-	-
	240	92.98	95.09	96.04	6.7	fusion	-	-
B	0	0	0	0	-	-		
(70°C)	30	76.42	80.61	85.45	-	-	-	-
	60	77.46	82.51	86.27	-	-	-	-
	90	81.38	86.44	88.72	-	-	-	-
	120	88.41	92.27	93.66	5.6	fusion	-	-
	150	92.25	95.26	96.00	9.8	fusion	-	-
	180	92.69	95.18	95.70	14.3	coalescence	5.0	-
	240	94.57	96.87	96.88	18.9	coalescence	14.4	4.5
F	0	0	0	0	-	-		
(80°C)	30	79.65	84.15	87.84	-	-	-	-
	60	81.88	86.95	89.26	-	-	-	-
	90	87.74	91.77	92.77	12.4	fusion	-	-
	120	91.72	94.95	95.22	16.4	coalescence	16.6	-
	150	92.33	95.73	95.51	21.4	coalescence	15.2	4.6
	180	93.66	96.73	96.37	24.9	coalescence	14.0	4.6
	240	96.65	100.00	98.21	37.3	bead formation	10.5	4.5-4.6

[a] Sty 92.5%, DVB 7.5%, BPO 0.5%, 240 rpm., Tol 100%, PVA 0.09%, Monomer: H_2O, 1:7

Table 4.4, and Figures 4.7- 4.9 show the effect of the reaction temperature as that the conversion increases due to at the higher temperatures, the initiation rate increases in addition to the crosslinking rate, and high initiation rates result more short polymer chains. At high temperatures, the rate constant increases according to Arrhenius equation.

The rates of decomposition of initiations can be conveniently expressed in terms of the initiator half-life ($t_{1/2}$) which is defined as the time for the concentration of I to decrease to one half its original value.

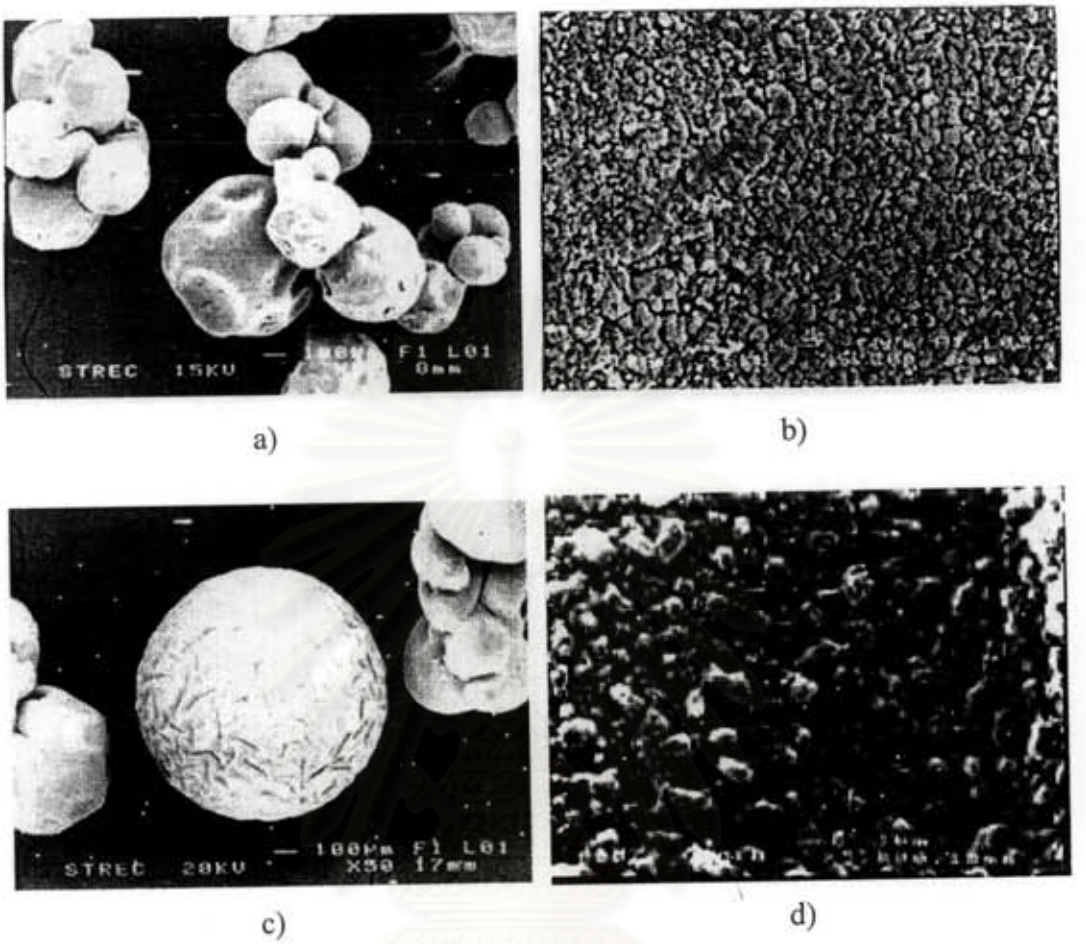

a) b)

c) d)

Figure 4.5. Scanning Electron Micrographs of the beads under the effect of the temperature: Sty 92.5%, DVB 7.5%, BPO 0.5%, 240 rpm., Tol 100%, PVA 0.09%, Monomer: H_2O, 1:7 at 240 min. of the reaction time.

a) Sample B: 70°C (x 50) b) Sample B: 70°C (x 5000)

c) Sample F: 80°C (x 50) d) Sample F: 80°C (x 5000)

ศูนย์วิทยทรัพยากร
จุฬาลงกรณ์มหาวิทยาลัย

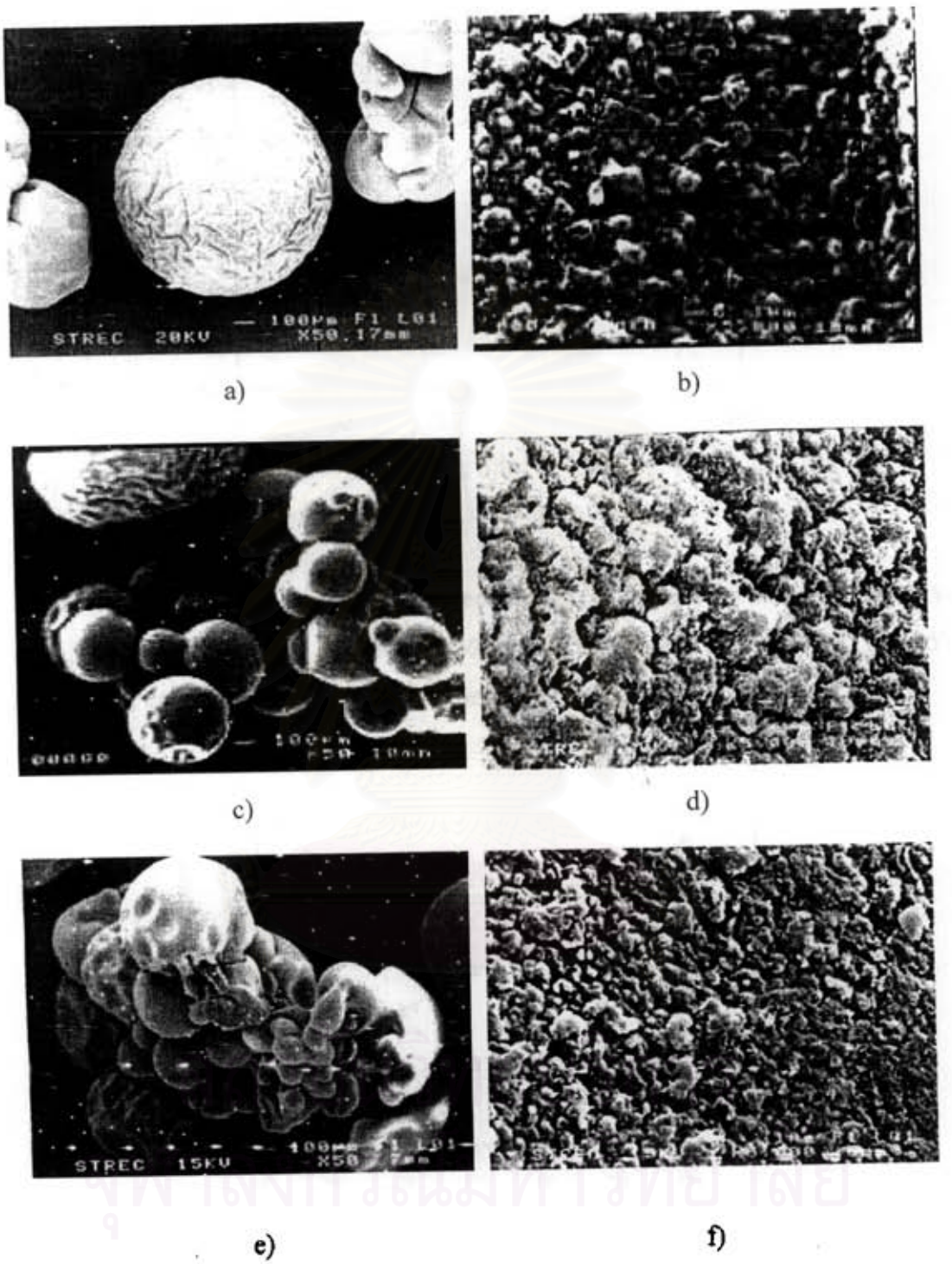

a) b)

c) d)

e) f)

Figure 4.6. Scanning Electron Micrographs of Sample F: Sty 92.5%, DVB 7.5%, 80°C, BPO 0.5%, 240 rpm., Tol 100%, PVA 0.09%, Monomer: H_2O, 1:7

a) at 240 min. (x 50)
b) at 240 min. (x 5000)
c) at 180 min. (x 50)
d) at 180 min. (x 5000)
e) at 150 min. (x 50)
f) at 150 min. (x 5000)

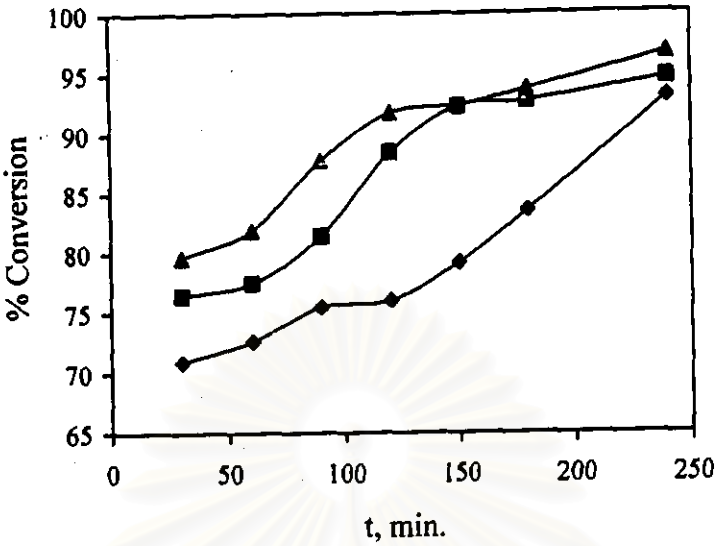

Figure 4.7 Effect of the temperature on conversion of styrene monomer; (The curves ♦♦♦, ■■■, and ▲▲▲ are for temperature 60, 70, and 80°C; when Sty 92.5%, DVB 7.5%, BPO 0.5%, 240 rpm., Tol 100%, Monomer: H_2O, 1:7; are used).

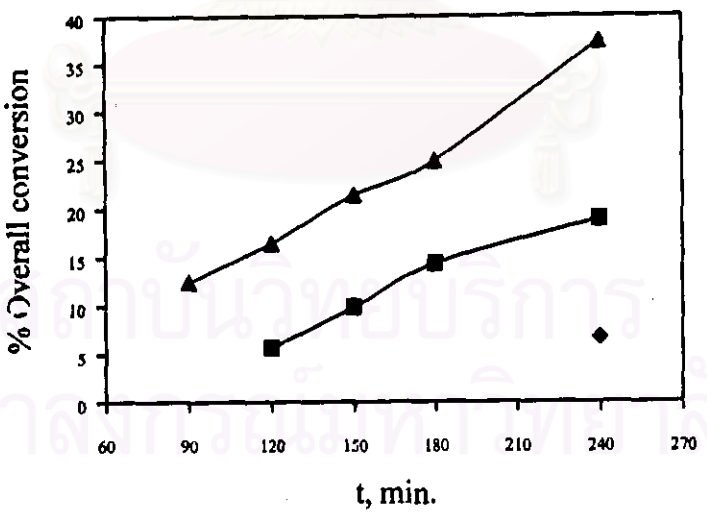

Figure 4.8 Effect of the temperature on overall conversion of styrene-divinylbenzene; (The curves ♦♦♦, ■■■, and ▲▲▲ are for temperature 60, 70, and 80°C; when Sty 92.5%, DVB 7.5%, BPO 0.5%, 240 rpm., Tol 100%, Monomer: H_2O, 1:7; are used).

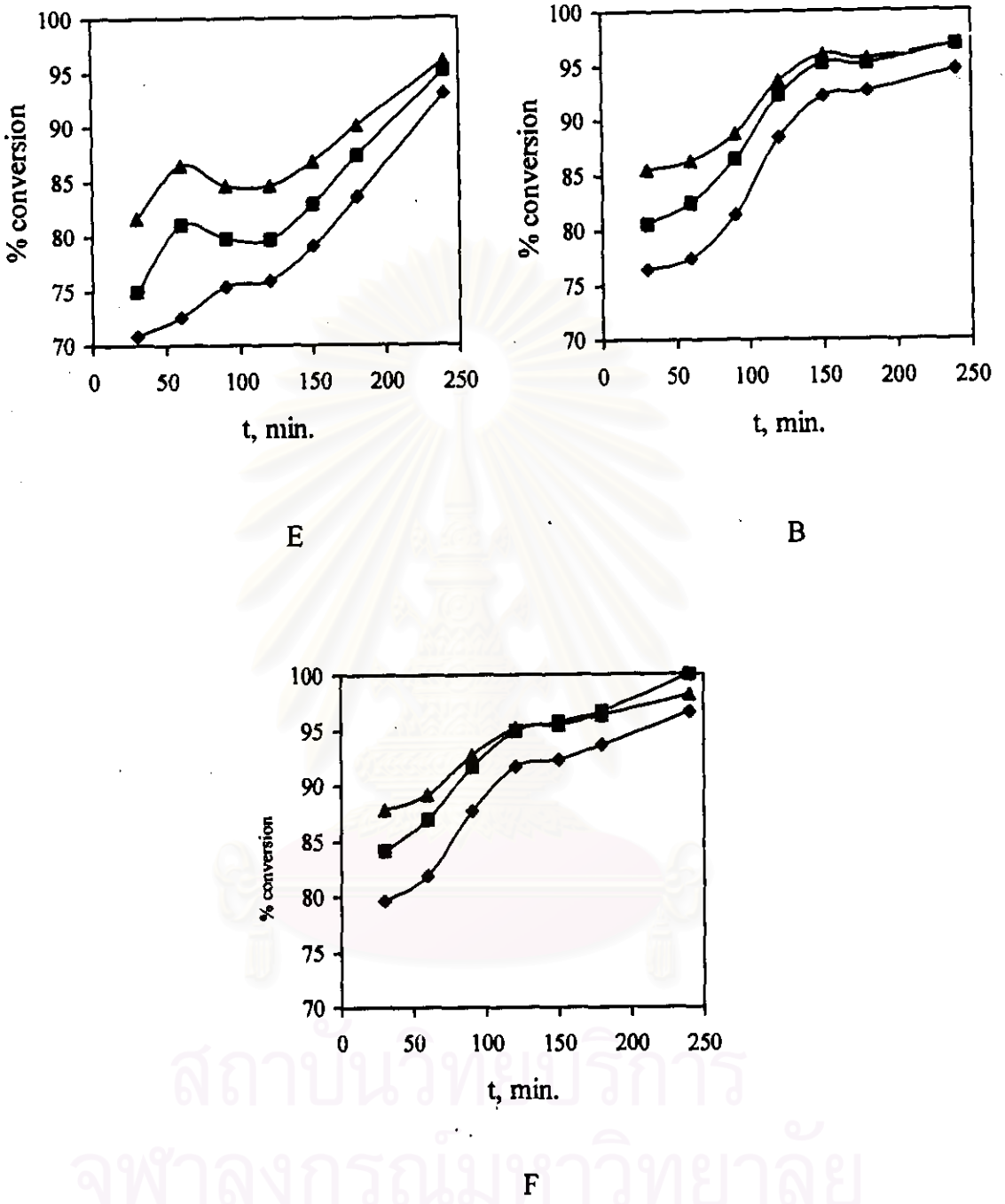

Figure 4.9 Effect of the temperature on conversion of individual monomers (The curves ◆◆◆, ■■■, and ▲▲▲ are for Sty, DVB, and EVB; when Sty 92.5%, DVB 7.5%, Tol 100%, Monomer: H_2O, 1:7, BPO 0.5%, 240 rpm., PVA 0.09%, temperature; Sample E (60°C), Sample B (70°C), Sample H (80°C)).

The rate of initiator disappearance is

$$-\frac{d[I]}{dt} = k_d[I] \qquad (4.1)$$

which on integration yields $[I] = [I]_o e^{-k_d t}$ or $\log\frac{[I]_o}{[I]} = k_d t$. Where $[I]_o$ is the initiator concentration at the start of polymerization $t_{1/2}$ is obtained as $t_{1/2} = \frac{0.693}{k_d}$.

Half-life of benzoyl peroxide is reduced when temperature is high. The effect of temperature on the rate and degree of polymerization is of prime importance in determining the manner of performing a polymerization. Increasing the reaction temperature usually increases the polymerization rate. However, the quantitative effect of temperature is complex since R_p depend on a combination of three rate constants.

At higher temperature of 70°C and the reaction time of 240 minutes, the copolymer is can form beads (Figure 4.5). The higher temperature and longer reaction time allow more polymeric chains to propagate, crosslink, and form network which results in a formation of beads.

4.2.3 The effect of the agitation

The effect of the agitation was studied using the standard recipe shown in Table 3.1. Three runs (G, B and H) were carried out using three different agitations (180, 240, and 300 rpm.). The conversion of the individual monomers was followed by gas chromatographic technique which was shown in Table 4.5 and Figure 4.13. The overall conversion of polymer was determined gravimetrically which was then shown in Table 4.5 and Figure 4.12. The result shows that the conversion does not give a difference with the agitation. But it seen that the average particle sizes increased when the speed reduced from Table 4.6.

Table 4.5 Effect of the Agitation on Kinetics of Copolymerization of Styrene and Divinylbenzene.

Sample[a]	Time (min)	Conversion of individual monomer (%)			Overall conversion (%)	Morphology	Swelling Ratio	SEM in Figure
		Sty	DVB	EVB				
G	0	0	0	0	-	-		
(180 rpm.)	30	58.37	65.87	74.45	-	-	-	-
	60	69.04	76.32	81.64	-	-	-	-
	90	81.44	87.27	89.89	-	-	-	-
	120	82.72	88.34	90.49	4.4	fusion	-	-
	150	90.00	93.40	94.47	11.4	fusion	11.3	-
	180	92.40	95.03	95.72	13.0	fusion	13.1	-
	240	95.12	97.55	97.63	16.8	coalescence	13.1	4.10
B	0	0	0	0	-	-		
(240 rpm.)	30	76.42	80.61	85.45	-	-	-	-
	60	77.46	82.51	86.27	-	-	-	-
	90	81.38	86.44	88.72	-	-	-	-
	120	88.41	92.27	93.66	5.6	fusion	-	-
	150	92.25	95.26	96.00	9.8	fusion	-	-
	180	92.69	95.18	95.70	14.3	coalescence	5.0	-
	240	94.57	96.87	96.88	18.9	coalescence	14.4	4.10
H	0	0	0	0	-	-		
(300 rpm.)	30	77.52	82.37	87.03	-	-	-	-
	60	80.75	86.61	90.06	-	-	-	-
	90	84.63	89.52	92.30	-	-	-	-
	120	85.69	91.87	93.86	3.3	fusion	-	-
	150	91.18	94.73	95.85	8.0	fusion	-	-
	180	91.61	94.85	95.76	8.1	fusion	16.5	-
	240	93.37	95.99	96.41	14.4	coalescence	14.3	4.10

[a] Sty 92.5%, DVB 7.5%, BPO 0.5%, 70°C, Tol 100%, PVA 0.09%, Monomer: H_2O, 1:7

Table 4.5, and Figures 4.11, 4.12 and 4.13 show that the agitation of the reaction increases, the conversion does not give a difference with agitation. The function of agitation is to develop size distribution and drop sizes of monomer phase during the reaction. The agitation rate in suspension polymerization determines the particle size distribution, as it causes the dispersion of the organic phase in the aqueous phase. Assumption was made as that the extent of agitation is sufficient to maintain a uniform level of turbulence throughout the reactor so that the mean drop sizes and the size distribution are the same throughout.

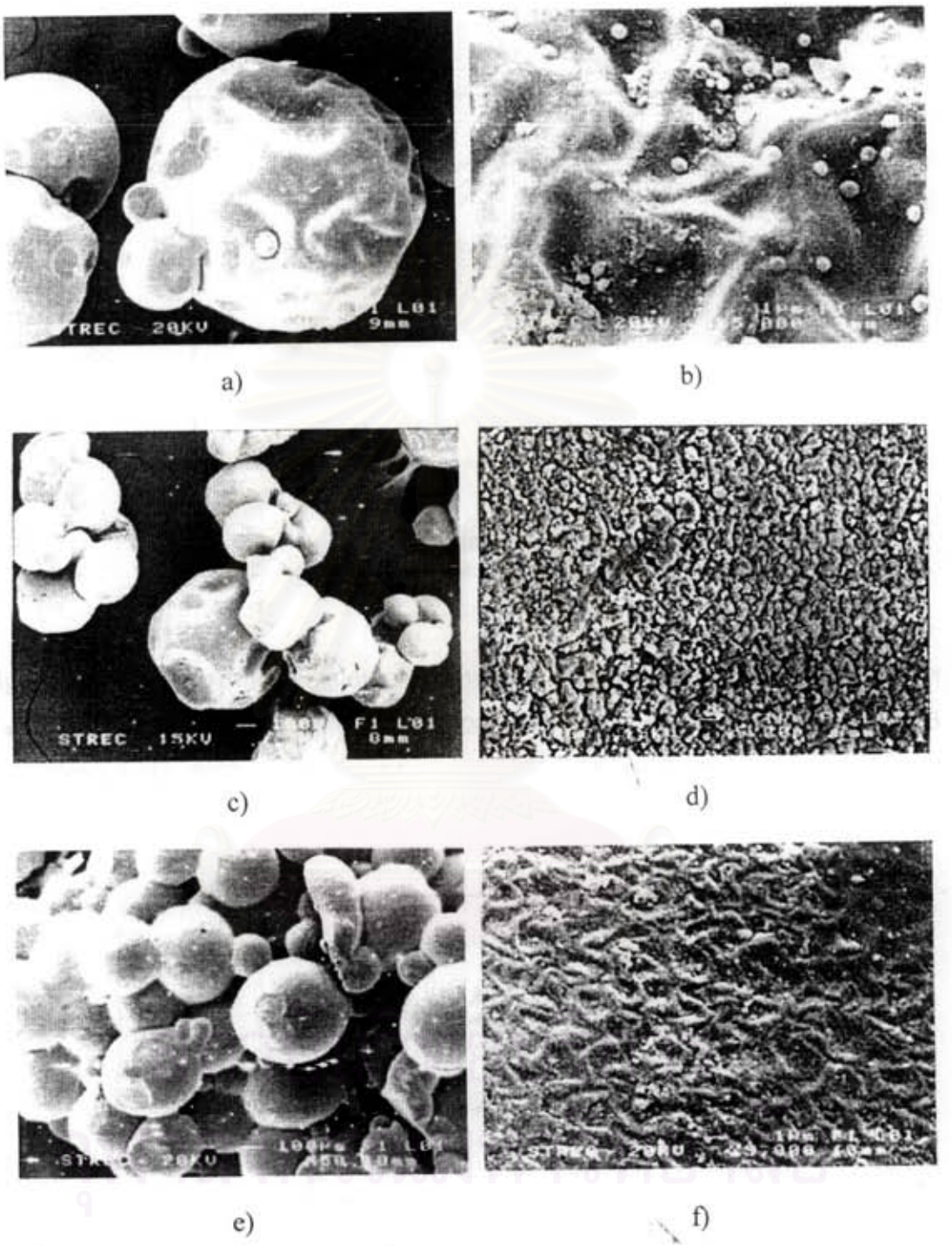

Figure 4.10. Scanning Electron Micrographs of the beads under the effect of the agitation : Sty 92.5%, DVB 7.5%, 70°C, BPO 0.5%, Tol 100% PVA 0.09%, Monomer: H_2O, 1:7 at 240 min. of the reaction time.

a) Sample G: 180 rpm (x 50)
b) Sample G: 180 rpm (x 5000)
c) Sample B: 240 rpm (x 50)
d) Sample B: 240 rpm (x 5000)
e) Sample H: 300 rpm (x 50)
f) Sample H: 300 rpm (x 5000)

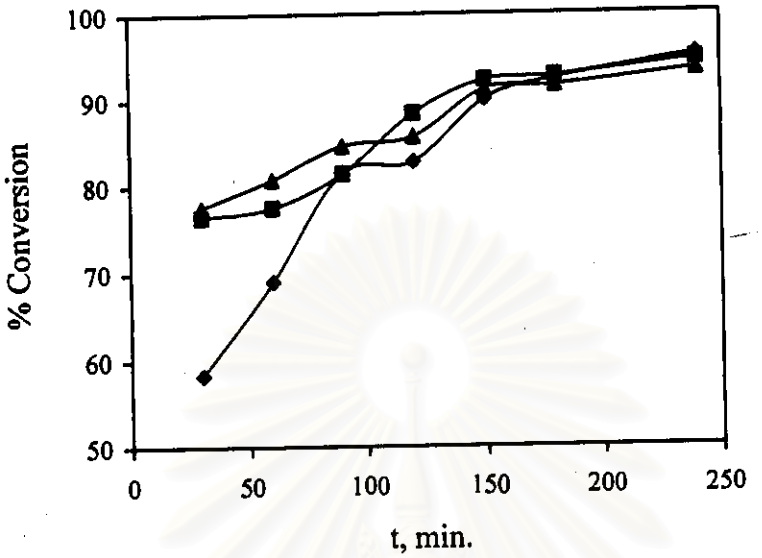

Figure 4.11 Effect of the agitation on conversion of styrene monomer; (The curves ♦♦♦, ■■■, and ▲▲▲ are for agitation 180, 240, and 300 rpm.; when Sty 92.5%, DVB 7.5%, BPO 0.5%, 70°C, Tol 100%, Monomer: H_2O, 1:7; are used).

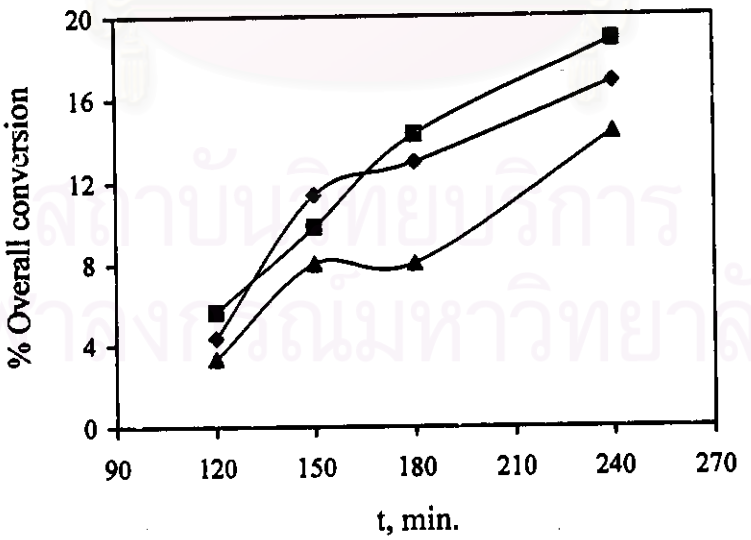

Figure 4.12 Effect of the agitation on overall conversion of styrene-divinylbenzene; (The curves ♦♦♦, ■■■, and ▲▲▲ are for agitation 180, 240, and 300 rpm.; when Sty 92.5%, DVB 7.5%, BPO 0.5%, 70°C, Tol 100%, Monomer: H_2O, 1:7; are used).

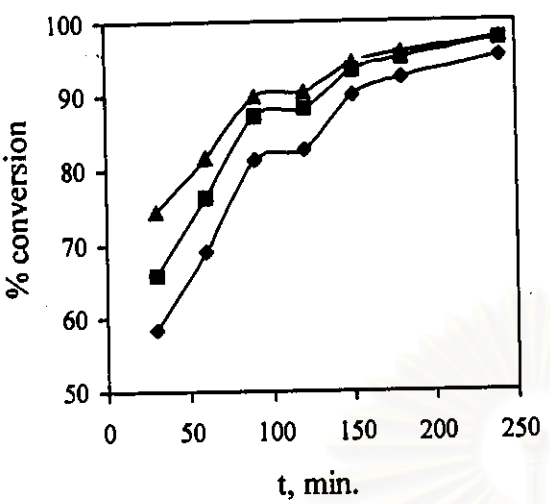

G

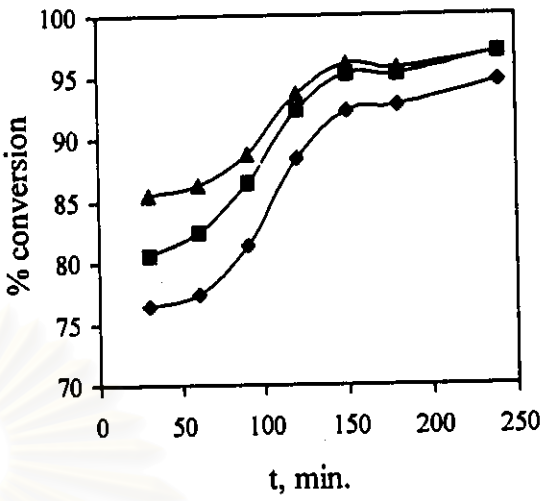

B

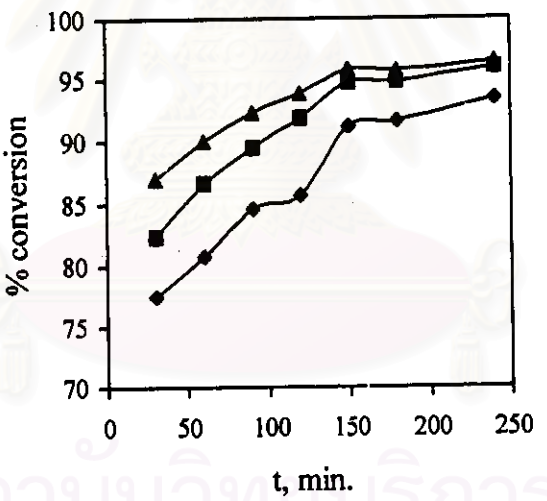

H

Figure 4.13 Effect of the agitation on conversion of individual monomers (The curves ♦♦♦, ■■■, and ▲▲▲ are for Sty, DVB, and EVB; when Sty 92.5%, DVB 7.5%, 70°C., Tol 100%, Monomer: H_2O, 1:7, BPO 0.5%, PVA 0.09%, agitation; Sample G (180 rpm.), Sample B (240 rpm.), Sample H (300 rpm.)).

When two immiscible liquids are agitated, a dispersion of one liquid in the other is formed. In the absence of sufficient concentrations of suspension stabilizers, continuous breakage and coalescence of droplets occur until, after a short time, a dynamic equilibrium is established. At equilibrium, the breakage and coalescence occur at the same rate, and the average size and the size distribution of the drops are governed by the type and extent of agitation and the physical properties of the two liquids. Under turbulent conditions, breakage occurs due to turbulent velocity and pressure variations along the surface of the drop. The coalescence occurs due to the collision of drops in a turbulent field, some of these collisions resulting in coalescence. When stabilizers are used, the coalescence efficiency, which is defined as the fraction of collisions resulting in coalescence, is close to unity, is reduced as the stabilizer adsorb on the surface of the drops. As the bulk concentration of the stabilizer is increased, its surface concentration increases and coalescence efficiency decreases until, at a certain surface coverage, called the critical surface coverage, the coalescence is completely eliminated. Above this coverage the dispersion is noncoalescing. Table 4.6 shows relation of agitation and particle sizes. When the agitation of the reaction increases, the particle sizes decreases [23].

From the McManamey formular [23]

$$d = const(\sigma / \rho_c)N^{-6/5}D^{-4/5} \tag{4.2}$$

where d is mean diameter, N is the speed of agitation, D is the diameter of the agitator, σ is the interfacial tension and ρ_c is the continuous phase density. These show, if D, σ, ρ_c parameters are constant, diameter of particle depends on the speed of agitation. These speeds increase, the shear force is increased too.

Table 4.6 Relation of agitation and particle sizes of Samples G, B, and H at 240 min.

Agitation (rpm.)	Particle sizes (mm.)
180	0.9410
240	0.7764
300	0.4444

Figure 4.10 show that the polymer formed was coalesced the higher the agitation speed, the more the coalescence of the polymer beads.

4.2.4 The effect of the crosslinking agent

The effect of the crosslinking agent was studied using the standard recipe shown in Table 3.1. Three runs (I, B and J) were carried out using three different crosslinking agent concentrations (%DVB of 5.0, 7.5. and 10.0 based on monomer phase). The conversion of the individual monomers was followed by gas chromatographic technique which was shown in Table 4.7 and Figure 4.17. The overall conversion of polymer was determined gravimetrically which was then shown in Table 4.7 and Figure 4.16.

Table 4.7, and Figures 4.15, 4.16 and 4.17 show that the conversion does not give a difference with the crosslinking monomer concentration.

ศูนย์วิทยทรัพยากร
จุฬาลงกรณ์มหาวิทยาลัย

Table 4.7 Effect of the Crosslinking Agent Concentration on Kinetics of Copolymerization of Styrene and Divinyibenzene.

Sample[a]	Time (min)	Conversion of individual monomer (%)			Overall conversion (%)	Morphology	Swelling Ratio	SEM in Figure
		Sty	DVB	EVB				
I	0	0	0	0	-	-		
(DVB 5%)	30	75.45	83.53	85.16	-	-	-	-
	60	77.77	85.50	86.25	-	-	-	-
	90	80.72	87.47	87.95	-	-	-	-
	120	81.77	89.43	89.74	-	-	-	-
	150	87.42	93.66	93.79	-	-	-	-
	180	90.53	95.56	95.50	10.6	fusion	-	-
	240	95.87	100.00	98.02	15.0	fusion	13.1	-
B	0	0	0	0	-	-		
DVB 7.5%)	30	76.42	80.61	85.45	-	-	-	-
	60	77.46	82.51	86.27	-	-	-	-
	90	81.38	86.44	88.72	-	-	-	-
	120	88.41	92.27	93.66	5.6	fusion	-	-
	150	92.25	95.26	96.00	9.8	fusion	-	-
	180	92.69	95.18	95.70	14.3	coalescence	5.0	-
	240	94.57	96.87	96.88	18.9	coalescence	14.4	4.14
J	0	0	0	0	-	-		
(DVB 10%)	30	70.57	76.51	81.86	-	-	-	-
	60	76.85	81.44	86.00	-	-	-	-
	90	81.02	85.87	88.61	-	-	-	-
	120	85.74	90.34	92.05	10.5	fusion	-	-
	150	91.00	93.70	94.78	12.1	fusion	-	-
	180	93.23	95.41	96.04	14.7	coalescence	8.6	-
	240	94.25	96.44	96.60	18.1	coalescence	14.1	4.14

[a] BPO 0.5%, 70°C, 240 rpm., Tol 100%, PVA 0.09%, Monomer: H_2O, 1:7

At %DVB of 5.0, the polymeric beads formed were clustered, fused, and no bead formation could be observed due to that the crosslinking agent usually helps stabilize and maintain the dimension of the bead. Thus, the small amount of the crosslinking agent is not sufficient to help the bead formation. Figure 4.14 shows that DVB concentration of 7.5 and 10.0 are sufficient for the bead formation with secondary nucleation. Organic phase inhibitor such as mono ethyl hydroquinone is suggested to add for suppression of the small beads.

Figure 4.14 C) shows that the beads are rather spherical with some dimple or dented surface, suggesting more DVB is needed.

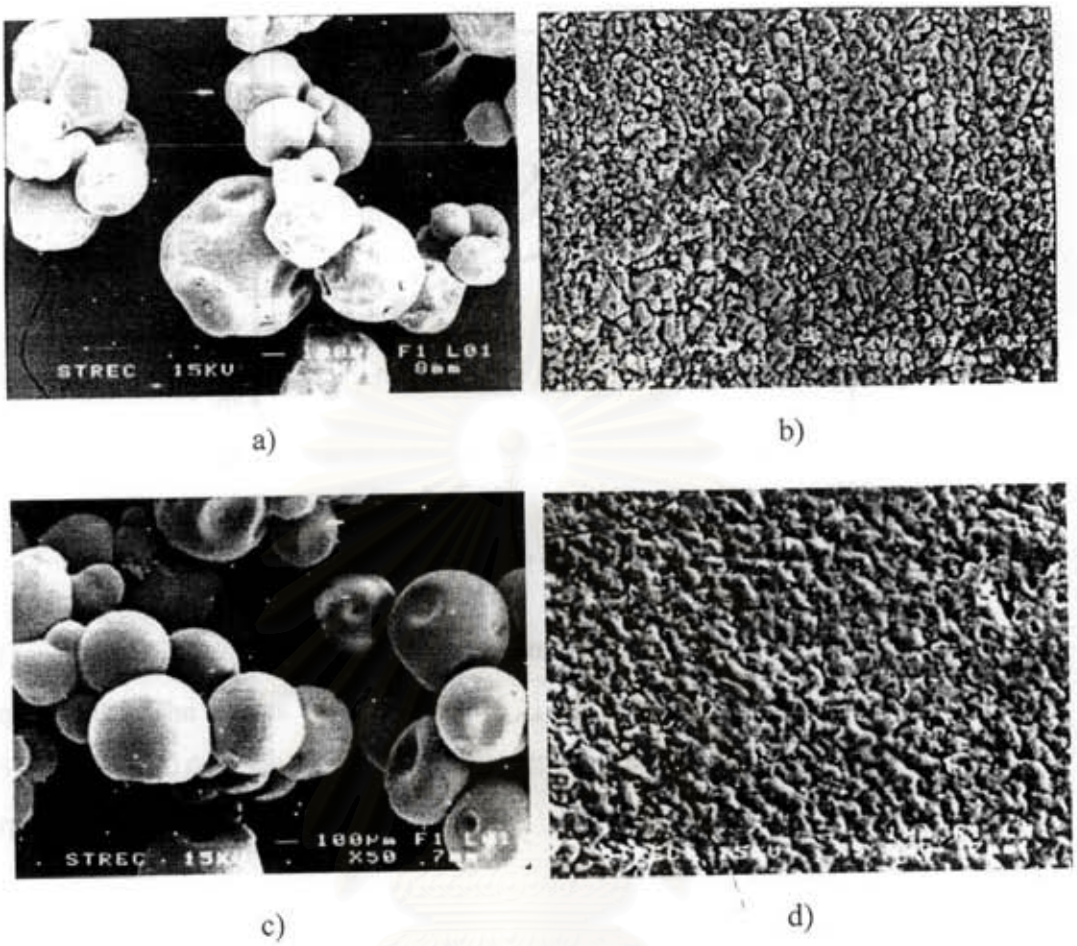

Figure 4.14. Scanning Electron Micrographs of the beads under the effect of the crosslinking agent: 70°C, BPO 0.5%, 240 rpm., Tol 100%, PVA 0.09%, Monomer: H_2O 1:7 at 240 min. of the reaction time.

a) Sample B: DVB 7.5% (x 50) b) Sample B: DVB 7.5% (x 5000)

c) Sample J: DVB 10.0% (x 50) d) Sample J: DVB 10.0% (x 5000)

สถาบันวิทยบริการ
จุฬาลงกรณ์มหาวิทยาลัย

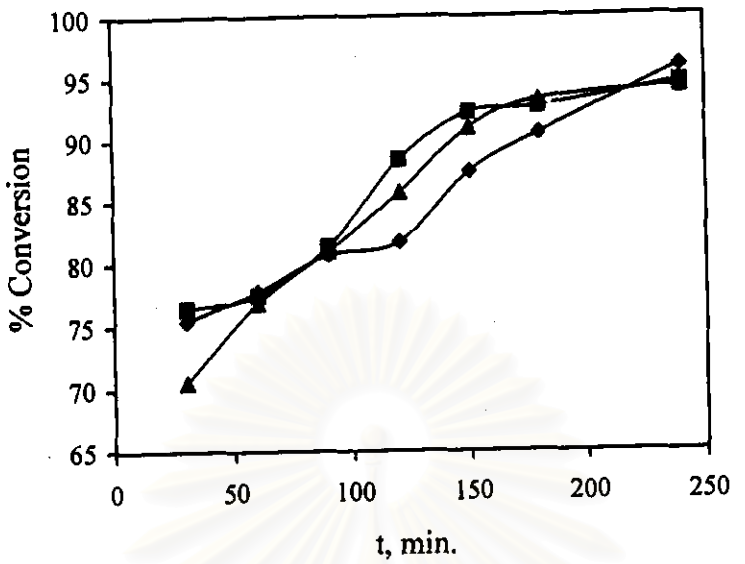

Figure 4.15 Effect of the corsslinking agent concentration on conversion of styrene monomer; (The curves ♦♦♦, ■■■, and ▲▲▲ are for corsslinking agent concentration 5.0, 7.5, and 10.0 % based on monomer phase; when BPO 0.5%, 70°C, Tol 100%, 240 rpm., Monomer: H_2O, 1:7; are used).

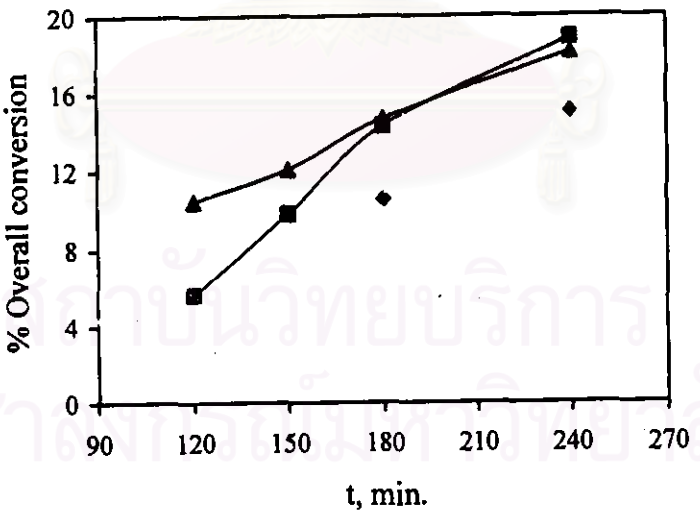

Figure 4.16 Effect of the corsslinking agent concentration on overall conversion of styrene - divinylbenzene; (The curves ♦♦♦, ■■■, and ▲▲▲ are for corsslinking agent concentration 5.0, 7.5, and 10.0 % based on monomer phase; when BPO 0.5%, 70°C, Tol 100%, 240 rpm., Monomer: H_2O, 1:7; are used).

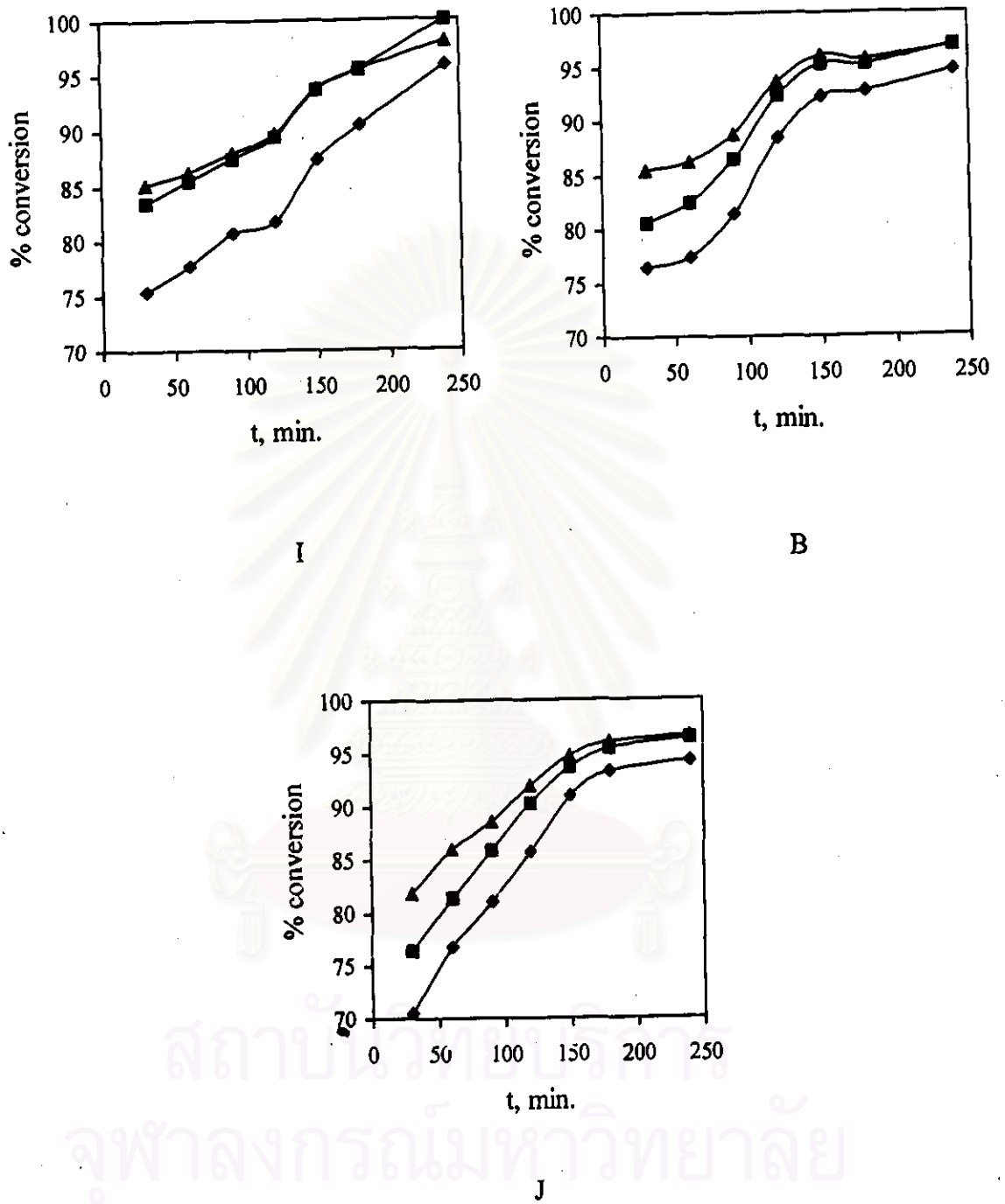

Figure 4.17 Effect of the crosslinking agent on conversion of individual monomers (The curves ◆◆◆, ■■■, and ▲▲▲ are for Sty, DVB, and EVB; when Tol 100%, Monomer: H_2O, 1:7, 70°C, BPO 0.5%, 240 rpm., PVA 0.09%, crosslinking agent; Sample I (DVB 5.0%), Sample B (DVB 7.5%), Sample J (DVB 10.0%)).

4.2.5 The effect of the diluent concentration

The effect of the diluent concentration was studied using the standard recipe shown in Table 3.1. Three runs (K, L,B and M) were carried out using four different dilutions as %toluene of 20, 60, 100 or 140 based on monomer phase. The conversion of the individual monomers was followed by gas chromatographic technique shown in Table 4.8 and Figure 4.23. The overall conversion of polymer was determined gravimetrically which was then shown in Table 4.8 and Figure 4.22.

Table 4.8, and Figures 4.21, 4.22 and 4.23 show that the conversion decreases due to the increase the diluent content by the diluents solvating the kinetic chains become less entangled. Due to the solvency power of toluene towards the copolymer of styrene-divinylbenzene, the surface of the copolymer becomes soften which may possibly stick the other beads together to precipitate as a lump.

The higher the solvency concentration, the greater the shorter kinetic chain because of the different concentration gradient and the similar interface. Likewise, the greater the diluent content, the more the coagulation. Thermodynamically, one possible cause for the coalesced copolymer could be the diluent concentration inside the reaction vessel.

Since the solubility parameters of toluene, styrene and divinylbenzene monomer with respect to the copolymer are very close ($\delta_{Toluene}$= 18.2, δ_{Sty}=19.0, δ_{DVB}= 17.2 and $\delta_{Sty\text{-}DVB}$= 18.6 $(MPa)^{1/2}$)[26], solvation, dilution, and droplet formation occur simultaneously.

A large number of monomer droplets were generated and distributed throughout the system, while the liquid medium responsible for the heat transfer was consequently reduced. It caused the accumulated heat inside the vessel and the small beads are forced to coagulate.

Table 4.8 Effect of the Diluent Concentration on Kinetics of Copolymerization of Styrene and Divinylbenzene.

Sample[a]	Time (min)	Conversion of individual monomer (%)			Overall conversion (%)	Morphology	Swelling Ratio	Figure of SEM
		Sty	DVB	EVB				
K	0	0	0	0	-	-		
(Tol 20%)	30	80.53	83.93	87.80	-	-	-	-
	60	83.39	87.42	90.12	-	-	-	-
	90	89.33	91.90	93.39	8.0	coalescence	-	4.19
	120	92.51	94.91	95.65	11.5	coalescence	12.6	-
	150	93.70	96.09	96.36	15.5	coalescence	13.6	4.19
	180	96.91	98.07	97.89	19.9	coalescence	12.3	-
	240	98.07	100.00	100.00	29.4	coalescence	8.6	4.18-4.19
L	0	0	0	0	-	-		
(Tol 60%)	30	76.39	81.07	85.58	-	-	-	-
	60	78.93	83.67	87.12	-	-	-	-
	90	85.15	89.46	91.54	6.1	fusion	-	-
	120	90.61	93.61	94.67	11.2	fusion	-	-
	150	94.22	96.46	96.92	12.3	fusion	12.7	-
	180	94.93	96.93	97.08	15.7	coalescence	14.3	4.20
	240	95.49	97.72	97.60	20.3	coalescence	12.7	4.18-4.20
B	0	0	0	0	-	-		
(Tol 100%)	30	76.42	80.61	85.45	-	-	-	-
	60	77.46	82.51	86.27	-	-	-	-
	90	81.38	86.44	88.72	-	-	-	-
	120	88.41	92.27	93.66	5.6	fusion	-	-
	150	92.25	95.26	96.00	9.8	fusion	-	-
	180	92.69	95.18	95.70	14.3	coalescence	5.0	-
	240	94.57	96.87	96.88	18.9	coalescence	14.4	4.18
M	0	0	0	0	-	-		
(Tol 140%)	30	50.16	58.58	67.58	-	-	-	-
	60	62.14	69.96	76.19	-	-	-	-
	90	67.11	72.93	78.94	-	-	-	-
	120	71.37	80.08	83.25	-	-	-	-
	150	75.67	85.40	87.91	-	-	-	-
	180	84.20	89.60	90.79	10.9	fusion	14.2	-
	240	93.10	95.55	95.90	13.9	fusion	15.0	-

[a] Sty 92.5%, DVB 7.5%, BPO 0.5%, 70°C, 240 rpm., PVA 0.09%, Monomer: H_2O, 1:7

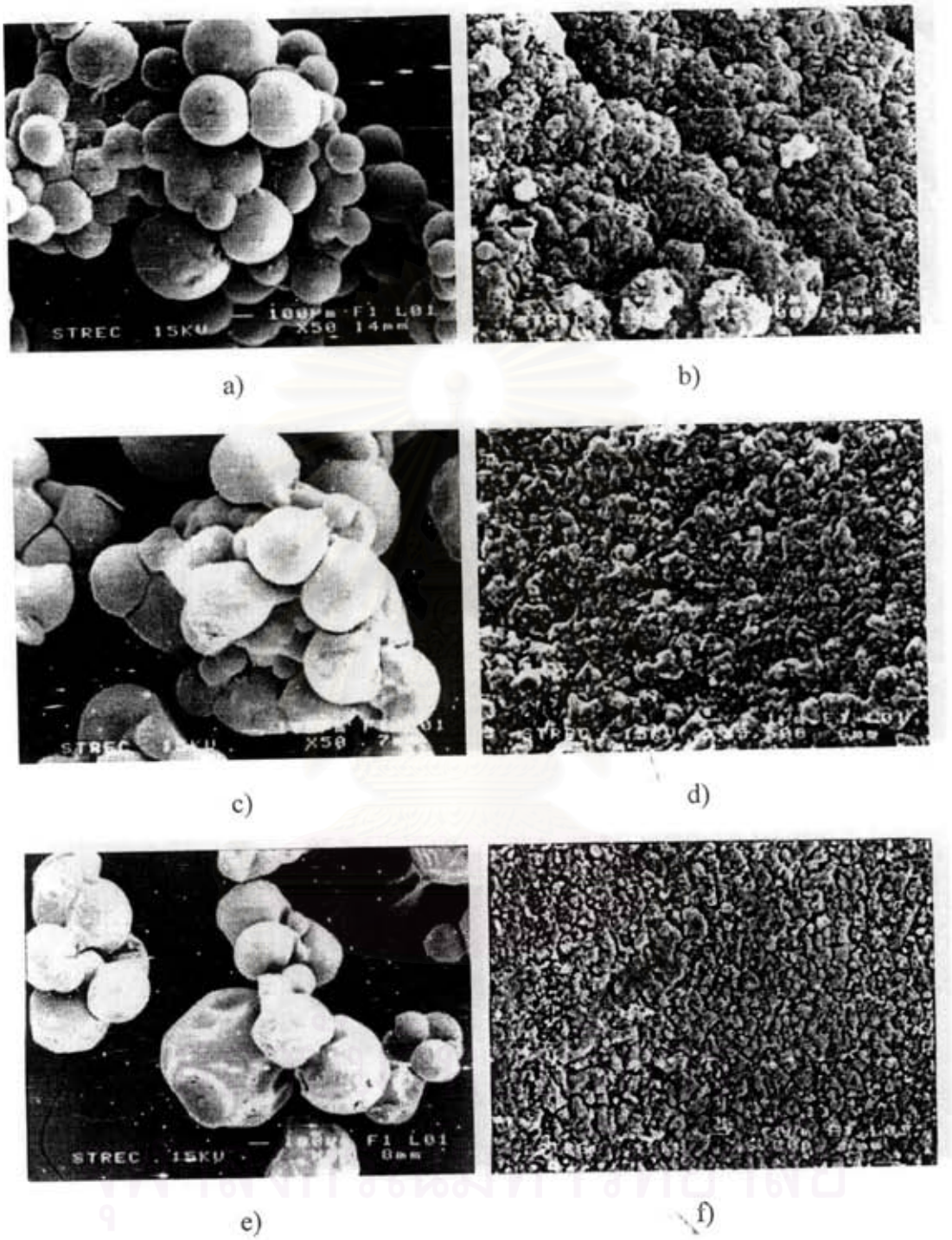

Figure 4.18. Scanning Electron Micrographs of the beads under the effect of the diluent concentration: Sty 92.5%, DVB 7.5%, BOP 0.5%, 70°C, 240 rpm., PVA 0.09%, Monomer: H_2O 1:7 at 240 min. of the reaction time.

a) Sample M: Tol 20% (x 50)
b) Sample M: Tol 20% (x 5000)
c) Sample L: Tol 60% (x 50)
d) Sample L: Tol 60% (x 5000)
e) Sample B: Tol 100% (x 50)
f) Sample B: Tol 100% (x 5000)

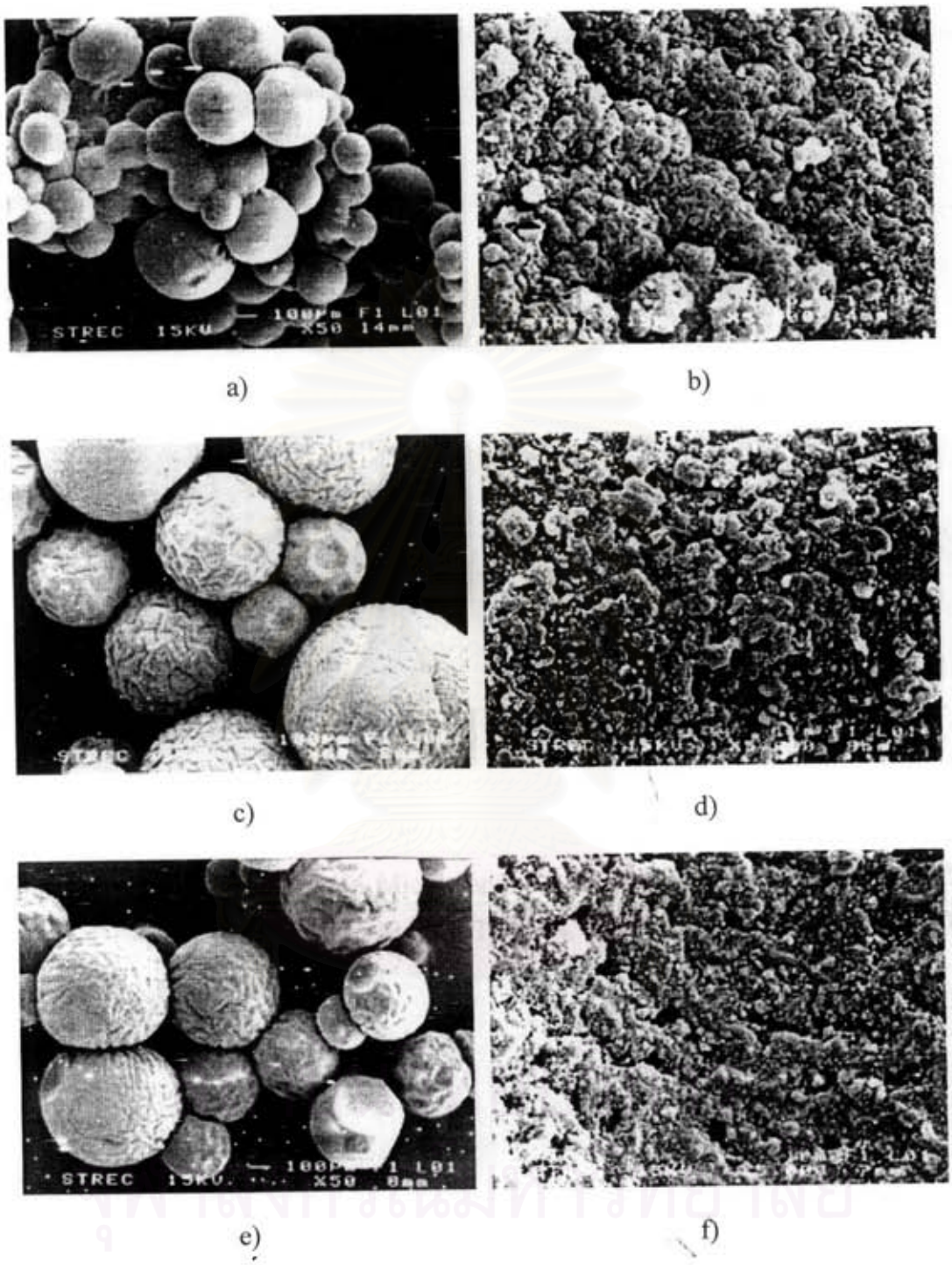

Figure 4.19. Scanning Electron Micrographs of Sample K: Sty 92.5%, DVB 7.5%, 70°C, BPO 0.5%, 240 rpm., Tol 20%, PVA 0.09%, Monomer: H_2O, 1:7

a) at 240 min. (x 50)
b) at 240 min. (x 5000)
c) at 150 min. (x 50)
d) at 150 min. (x 5000)
e) at 90 min. (x 50)
f) at 90 min. (x 5000)

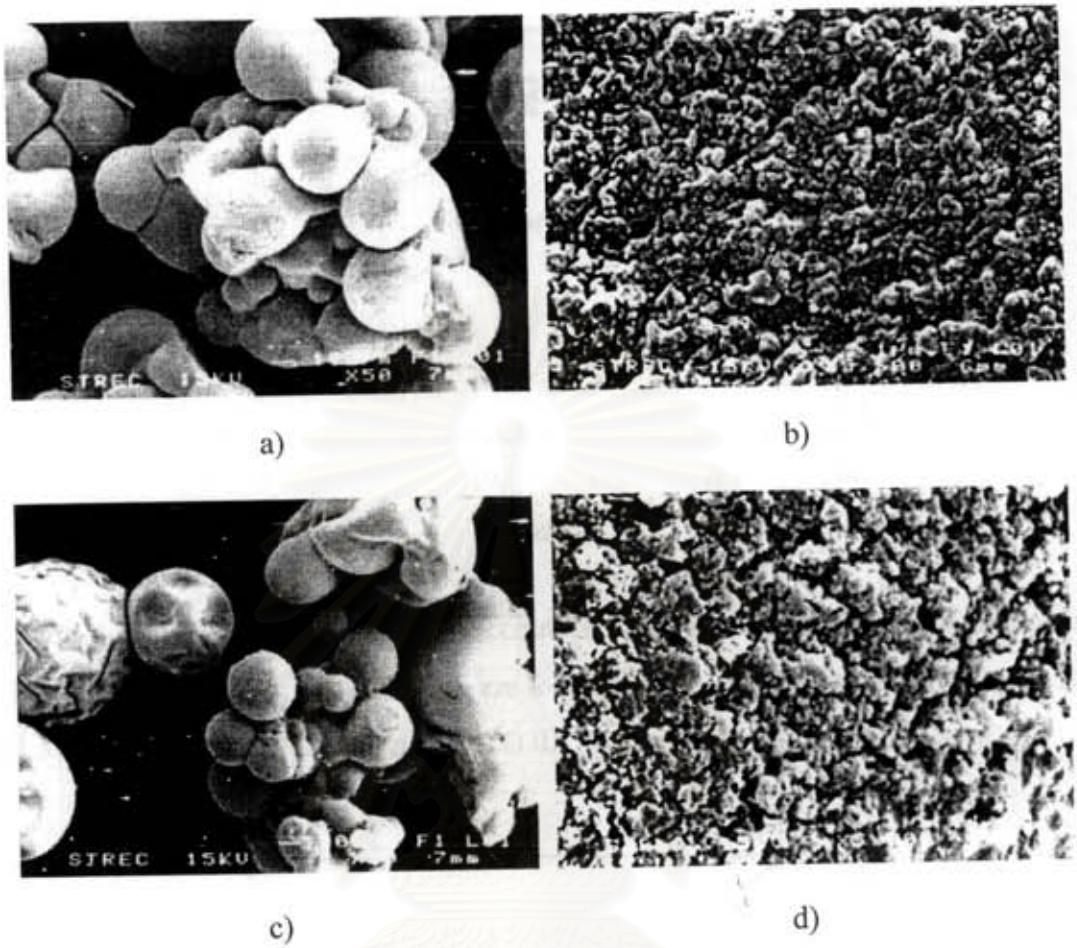

a) b)

c) d)

Figure 4.20. Scanning Electron Micrographs of Sample L: Sty 92.5%, DVB 7.5%, 70°C, BPO 0.5%, 240 rpm., Tol 60%, PVA 0.09%, Monomer: H_2O 1:7.

a) at 240 min. (x 50) b) at 240 min. (x 5000)

c) at 180 min. (x 50) d) at 180 min. (x 5000)

สถาบันวิทยบริการ
จุฬาลงกรณ์มหาวิทยาลัย

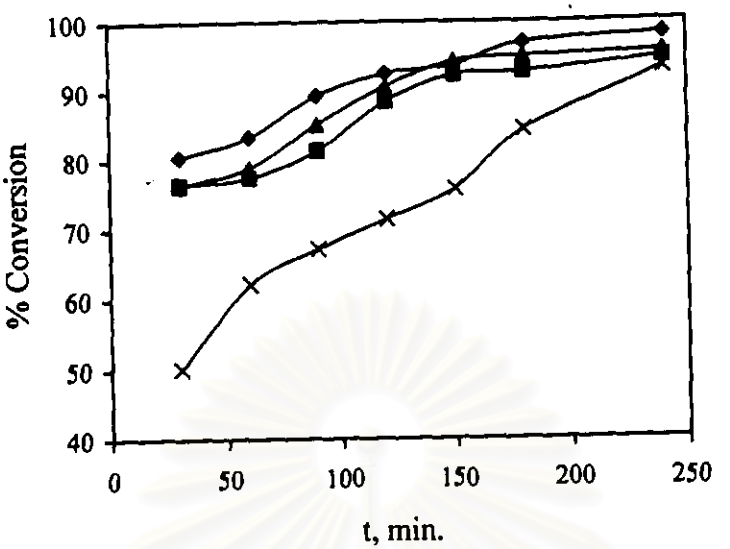

Figure 4.21 Effect of the diluent concentration on conversion of styrene monomer; (The curves ◆◆◆, ▲▲▲, ■■■, and ××× are for toluene 20, 60, 100, and 140%; when Sty 92.5%, DVB 7.5%, 70°C, 240 rpm., BPO 0.5%, Monomer: H_2O, 1:7; are used).

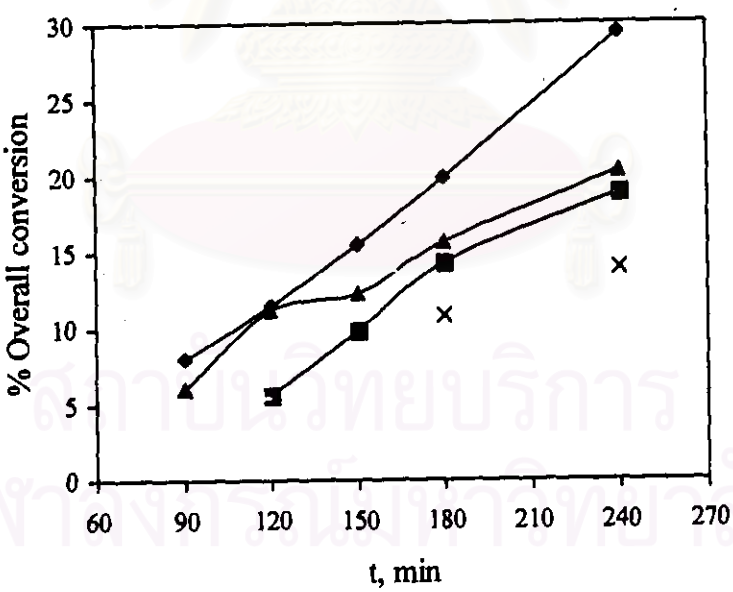

Figure 4.22 Effect of the diluent concentration on overall conversion of styrene - divinylbenzene; (The curves ◆◆◆, ▲▲▲, ■■■, and ××× are for toluene 20, 60, 100, and 140%; when Sty 92.5%, DVB 7.5%, 70°C, 240 rpm., BPO 0.5%, Monomer: H_2O, 1:7; are used).

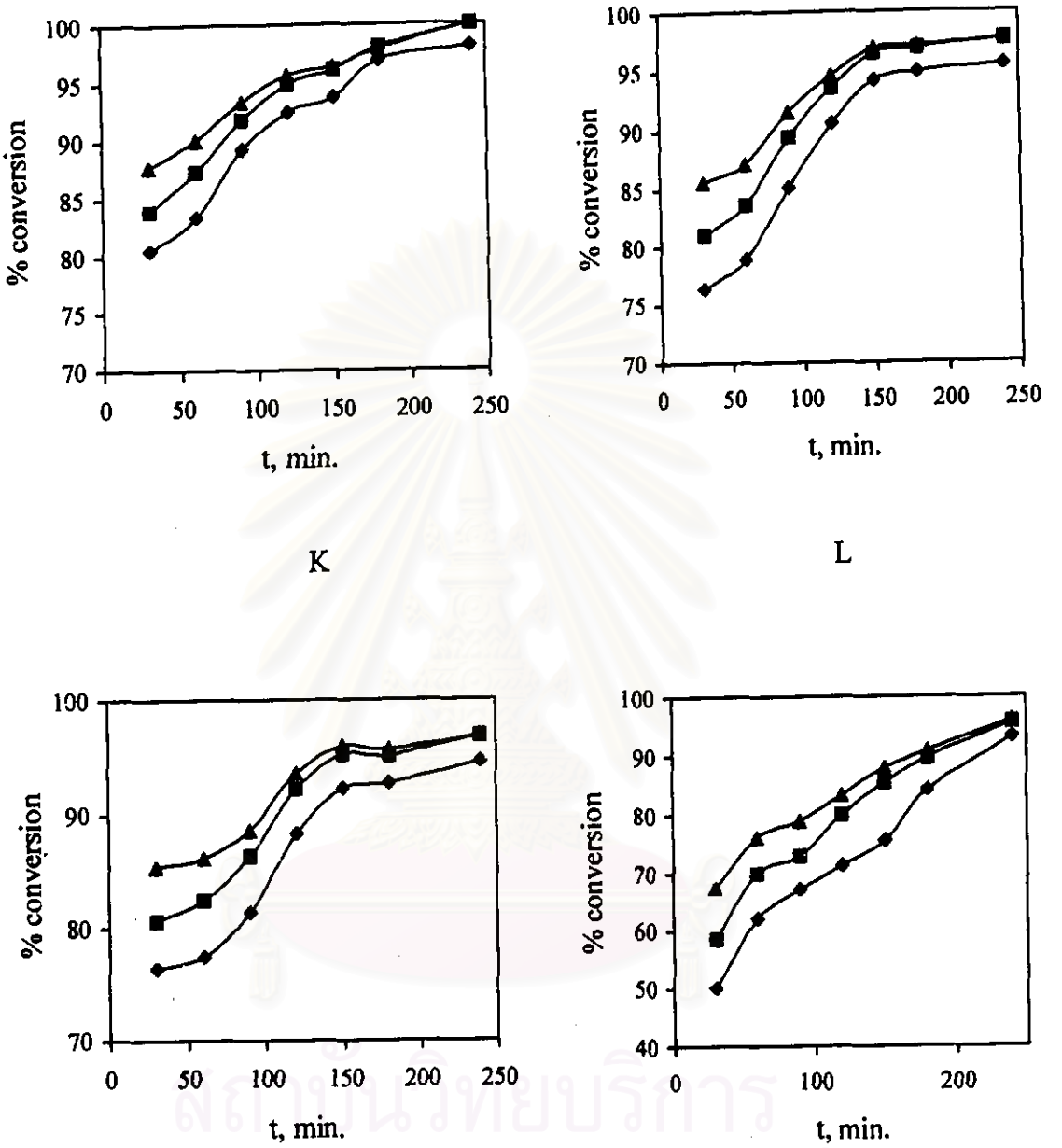

Figure 4.23 Effect of the diluent concentration on conversion of individual monomers (The curves ◆◆◆, ■■■, and ▲▲▲ are for Sty, DVB, and EVB; when Sty 92.5%, DVB 7.5%, Monomer: H_2O, 1:7, BPO 0.5%, 70°C, 240 rpm., PVA 0.09%, diluent concentration; Sample K (Tol 20%), Sample L (Tol 60%), Sample B (Tol 100%), Sample M (Tol 140%)).

4.3 Swelling properties

Swelling properties for the styrene-divinylbenzene copolymer is one of the almost application in various industries. Table 4.9 shows the swelling ratio of the styrene-divinylbenzene copolymer. In order to simplify the relation between the solvating power of the diluent and the styrene-divinylbenzene copolymer, the predictions using Hildebrand and three-dimensional solubility parameters will be discussed separately as method I and II.

Method I Hilderbrand solubility parameter [10]

The solubility parameter of styrene-divinylbenzene copolymer is 18.6 $(MPa)^{1/2}$. According to Hildebrand's theory a given diluent will be an ideally good solvent for the polymer when $|\delta_1 - \delta_2| \approx 0$ where δ_1 and δ_2 are the solubility parameters of solvent and solute, respectively. From Table 2.5, toluene is a good solvent for styrene-divinylbenzene copolymer chains with $|\delta_1 - \delta_2| = 0.4$ $(MPa)^{1/2}$.

Method II Three-dimensional solubility parameter [10]

For styrene-divinylbenzene copolymer, the center point coordinates and radius of the solubility sphere in the three-dimensional δ_d, δ_p, and δ_h space are 21.3, 5.8, 4.3 and 12.7 $(MPa)^{1/2}$, respectively. The diluent-polymer distances (R) were calculated using Eq. 2.20. If $R < 12.7$ the diluent will be a good solvent for Sty-DVB copolymer. As toluene, a well-known good solvent for styrene-divinylbenzene copolymer has R = 8.3 $(MPa)^{1/2}$.

Two methods show that "styrene-divinylbenzene copolymers can swell in toluene or other good solvents which has a solubility parameter of 18.6 $(MPa)^{1/2}$". The solvent uptake can appear in two ways: by filling the pores without affecting the gel regions (no volume change), and by chain displacement in the gel regions that causes bead expansion. The swelling of heterogeneous networks is governed by two separate processes [27]:

1. Solvation of network chains: The main driving force of this process is the changes in the free energies of mixing and elastic deformation during the expansion of the network. The extent of network solvation is determined by the cross-linking density of the network and by the interactions between solvent molecules and the network chains.
2. Filling of voids (pores) by the solvent: The extent of this process is determined by the total volume of (open) pores, i.e., by the volume of diluent separated out of the network phase during the polymerization.

Table 4.9 Swelling properties of styrene-divinylbenzene copolymers in toluene

Sample	Time (min.)	Swelling Ratio
B	180	5
	240	14
C	150	10
	180	7
	240	15
D	150	7
	180	9
	240	8
F	120	17
	150	15
	180	14
	240	10
G	150	11
	180	13
	240	13

Sample	Time (min.)	Swelling Ratio
H	180	16
	240	14
I	240	13
J	180	9
	240	14
K	120	13
	150	14
	180	12
	240	9
L	150	13
	180	14
	240	13
M	150	14
	180	15

4.3.1 The effect of the diluent concentration on swelling ratio

Figure 4.24 shows the swelling ratio for the styrene-divinylbenzene copolymers prepared at DVB concentration of 7.5 % using toluene as diluent with a dilution range of 20 to 140 %, based on monomer content. The swelling increased when the diluent concentration was increased. These results suggest that the increase of dilution with solvating diluents provokes enhancement of phase separation; after the diluent elimination, the total collapse of the micropores occurs, but in contact with solvent these pores will be reexpanded. Thus, the increase of dilution degree with solvating diluents enhances the phase separation and produces more flexible internuclear chains [2].

When Sample F synthesized with the condition as follows: %Sty 92.5, %DVB 7.5, %Tol 100, %BPO 0.5, 80°C, 240 rpm. at a function of times 240 , 180 , 150 and 120 min. was tested for its property which was show in Figure 4.25. Overall conversion increased the bead formation; and the swelling ratio decreases depending on reaction time. The swelling ratios were 17, 15, 14, and 10 for 120, 150, 180, and 240 min. of the reaction time, respectively. When the reaction time increase, the copolymer beads are more entangled and become less flexible leading to the decrease in swelling ratio.

Sample K synthesized with the condition as follows: %Sty 92.5, %DVB 7.5, %Tol 20, %BPO 0.5, 70°C, 240 rpm. at a function of times 240 , 180 , 150 and 120 min. was tested for its property which was show in Figure 4.26. Overall conversion increased the bead formation; and the swelling ratio decreases depending on reaction time. The swelling ratios were 13, 14, 12, and 9 for 120, 150, 180, and 240 min. of the reaction time, respectively. When the reaction time increase, the copolymer beads are more entangled and become less flexible leading to the decrease in swelling ratio.

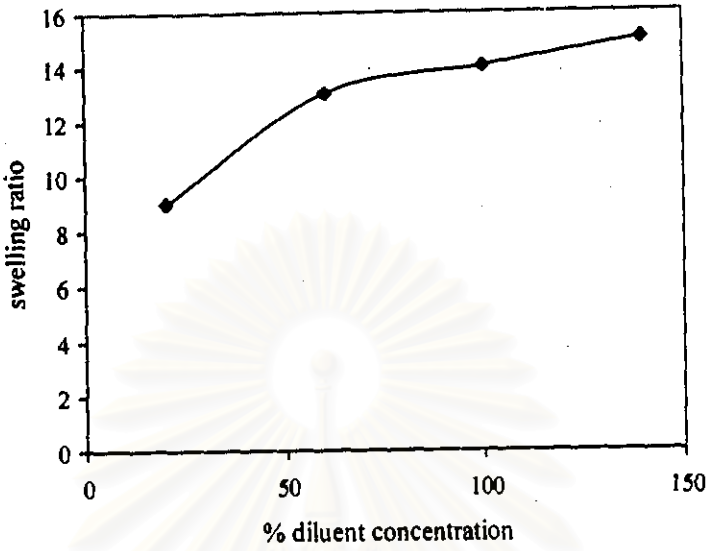

Figure 4.24. Degree of dilution with swelling ratio by using toluene and sample K, L, B, and M at 240 min.

สถาบันวิทยบริการ
จุฬาลงกรณ์มหาวิทยาลัย

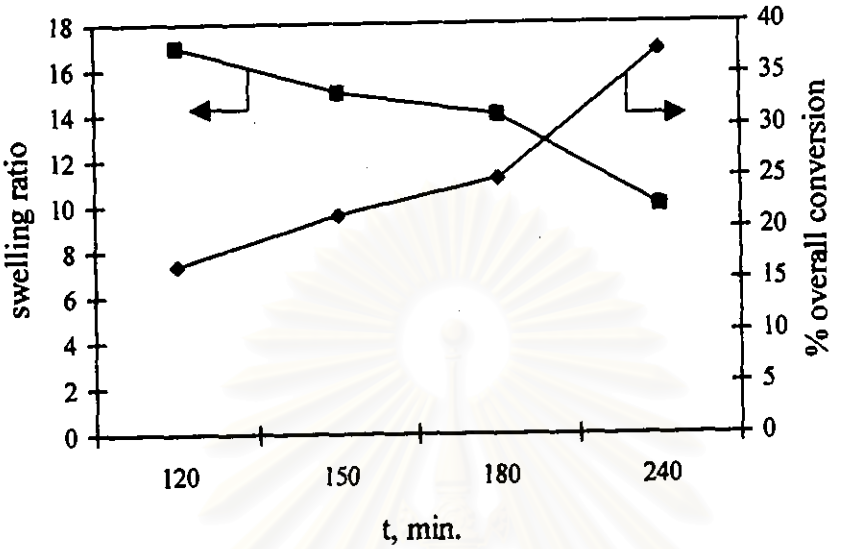

Figure 4.25. The plot of swelling ratio with % overall conversion on reaction time by Sample F (swelling ratio: ■■■, % overall conversion: ◆◆◆)

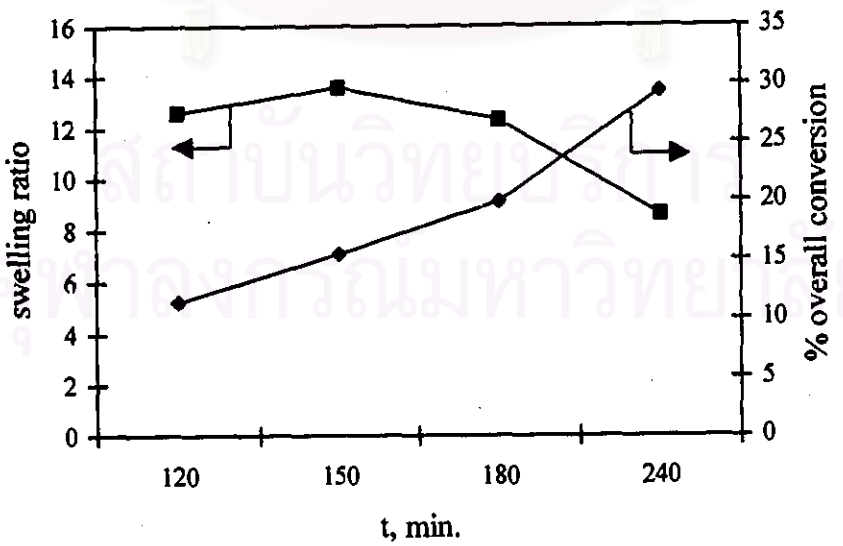

Figure 4.26. The plot of swelling ratio with % overall conversion on reaction time by Sample K (swelling ratio: ■■■, % overall conversion: ◆◆◆)

4.4 Mechanism of porous structure formation

Based on the observation of particle structure, a mechanism for pore formation during Sty-DVB copolymerization by suspension polymerization is proposed as a two-stage process [29].

4.4.1 The first stage in the formation of a macroporous structure is described by Kun and Kunin as a process consisting of three stages [30].

4.4.1.1 The first stage, each particle is composed of a solution of monomers, initiator, and the diluents; it is suspended in an aqueous solution and stabilized with surfactants. Since the DVB has a high reactivity ratio, during the very early stages of the polymerization DVB rich copolymer molecules are formed which are composed of straight chains with pendent vinyl groups [29] (During the early stages of reaction, yield so called "primary" macromolecules). When a bifunctional monomer molecule is attacked by a growing radical a pendent double bond is formed. When suck a pendent double bond reacts, in turn, a branch point is formed. Further reaction leads to the increase of intermolecular linkages, with the result of formation of small crosslinked nuclei of polymer molecules (the double bonds will yield to branch points connecting two chains) [18].

4.4.1.2 The second stage, continued polymerization yields intermolecularly crosslinked microgels and linear molecular chains that are soluble in the monomers. The monomers are transformed into crosslinked copolymer as the reaction proceeds; phase separation occurs between copolymer and linear polystyrene and diluent, which gives a copolymer-rich phase and a diluent-rich phase, the monomers being distributed between the two phases. Linear polymer used as diluent will be in a swollen state because the monomers themselves are good solvents. Since solvated and very lightly crosslinked copolymers can behave, in some respects, like a liquid, the interfacial tension at the polymer-rich phase gives it the low-energy spherical form, and the polymer is separated as a mass of microspheres [29].

4.4.1.3 The third stage, polymer macrogelation occurs and gives a gel type of particle composed of an agglomeration of microspheres. This is depicted schematically in Figure 4.27. The porous structure of these copolymers consists of globules; the smallest, rather spherical particles of about 100-200 Å in diameter are

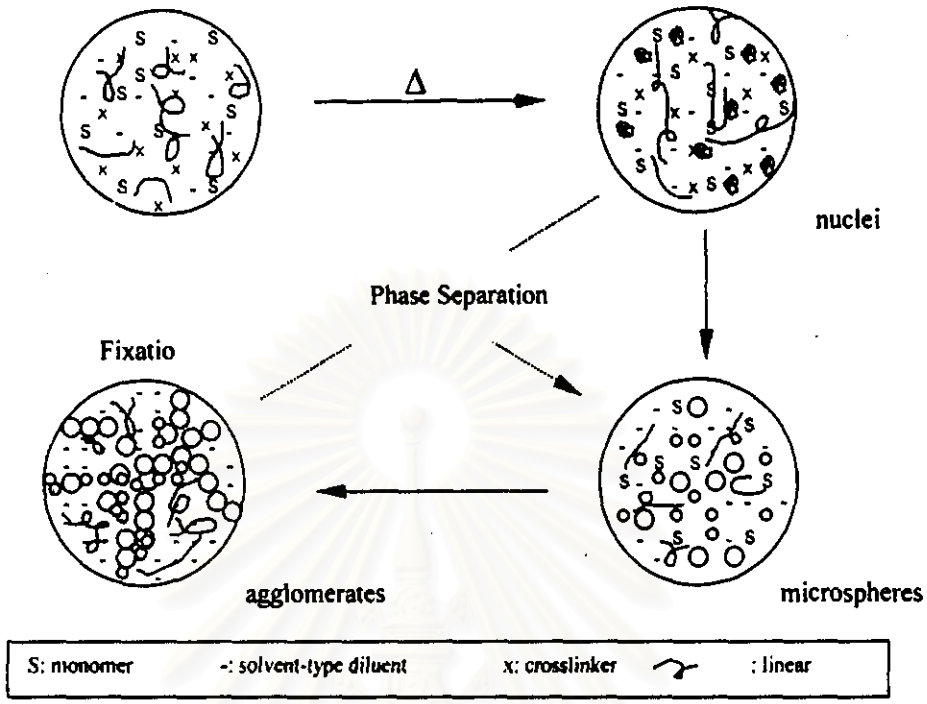

Figure 4.27. A schematic model for the process of pore formation in the copolymerization stage [29].

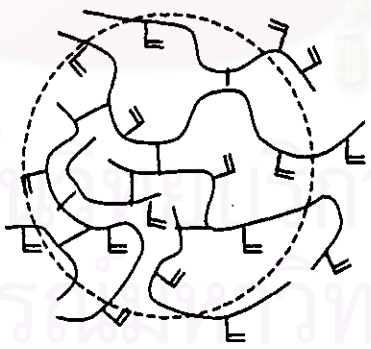

Figure 4.28. Schematic model of the internally compact crosslinked particles possessing microgel [32].

the "nuclei", and the aggregation of these nuclei results in the microspheres with diameters of 500-1000 Å; the microspheres are aggregated again in particles of about 2500-10,000 Å in diameter [31].

4.4.2 The second stage in pore-structure formation is the binding together and fixation of the microspheres and agglomerates. As the polymerization and formation of microspheres continue, the microspheres are bound together by the polymerization of the monomers, which have a higher percentage of monovinyl components in composition and act to solvate the microspherical polymers [29] (Primarily, compact internally crosslinked particles possessing microgel character are formed, which are linked through their peripheric double bonds to yield a gel [32]). Some fraction of the high molecular weight linear polystyrene is trapped within the microspheres and agglomerates while they are binding together; the inclusion of linear polymer is dependent on the nature of linear polymer and the extent of phase separation between the diluent phase and the copolymer phase. It is during this stage that the macroporous structure is actually formed. Voids between microspheres and agglomerates are filled with diluent. In the diluent phase, entanglement of linear polymer will take place, depending on the molecular weight of the polymer and interaction between solvent and linear polymer, thus explaining the sensitivity of the pore size distribution to the molecular weight of the linear polymer. After the removal of the diluents, polymer particles with macroporous structure are obtained [29].

4.5 Morphology of the surface of Sty-DVB copolymer

Direct observation of Sty-DVB copolymer morphology by scanning electron microscopy shows nodules of diameter in Samples B, C and D as shown in Figure 4.1. The beads in Samples B and F (Figures 4.5 - 4.6), Samples G, B and H (Figure 4.10), Samples B and J (Figure 4.14), and Samples K, L and B (Figures 4.18-4.20) which are of approximately 0.4-1 mm beads. Morphology of beads by solvating shows the following aspects: The beads were swollen in toluene implying that the polymer chains are less entangled and their nuclei are more expanded. Less compact macrospheres could result in due to the solvent in equilibrium with the swollen nuclei; and smaller agglomerates and macropores are anticipated. Good solvents produce

structures with small pores inside and on the surface. When the small polymer beads are dried, they stick together because the trapped solvent was evaporated through the surface.

4.5.1 The effect of the initiator concentration

Figure 4.1 shows the electron micrographs of the surface of Sty-DVB copolymer by effect of initiator concentration at the polymerization time of 240 min. The polymer cannot form beads but a sheet was obtained. The increase of the initiator concentration of BPO increase the surface of beads due to agglomeration of microspheres.

4.5.2 The effect of the temperature

Figure 4.5 shows the electron micrographs of the surface of Sty-DVB copolymer by effect of temperature (70 and 80°C) at the polymerization time of 240 min. Similar result was observed at 60°C polymerization. The increase in temperature in a solution reduces the surface tension and reduce the droplet formation and drop size. The higher the temperature, the lower the viscosity. The lower surface viscosity makes the beads stick together. Figure 4.6 shows the electron micrographs of the surface of Sty-DVB copolymer (Sample F) by variation of reaction times (240, 180, 150 min). The reaction times increases, the surface of beads are agglomerated from microspheres to macrospheres.

4.5.3 The effect of the agitation

Figure 4.10 shows the electron micrographs of the surface of Sty-DVB copolymer by effect of agitation at the polymerization time of 240 min. The copolymers prepared with lower agitation rates, have the large particle size with dimples or circular dents.

4.5.4 The effect of the crosslinking agent

Figure 4.14 shows the electron micrographs of the surface of Sty-DVB copolymer by effect of crosslinking agent concentration at the polymerization time of 240 min. The surfaces of beads are agglomerated by microspheres. DVB of 5%

content could not successfully from the beads due to the crosslinking monomer was not enough to run the reaction. The increase of crosslinking agent concentration exerted different effects on the heterogeneity of the copolymer surface and phase separation processes within the surface skin of the particles. The increase of the amount of crosslinking agent concentration produced a small effect on the surface porosity of the beads. The bead surfaces showed a tendency to be smooth [30].

4.5.5 The effect of the diluent concentration

Figure 4.18 shows the electron micrographs of the surface of Sty-DVB copolymer by effect of diluent concentration at the polymerization time of 240 min. The surfaces of beads were agglomerated by microspheres. When the diluent solvating power changes, the main differences on the porous structure formation are the critical concentrations for polymer precipitation during the early stages of polymerization, the tendency of precipitated polymer to agglomerate in microsphere and the entanglement degree of nuclear and internuclear chains. Polymer precipitation occurs earlier as the diluent solvating power. When diluent concentration decreases, microspheres on surface are more separated [30].

Figure 4.19 shows the electron micrographs of the surface of Sty-DVB copolymer of Sample K by variation of reaction times (240, 150, 90 min). The surface of beads were agglomerated by microspheres. The reaction times increase, the surfaces of beads are increased by the agglomeration of microspheres. Because of the less toluene content (20%) the entanglements between the polymer chains increase and the nuclei are aggregated into microspheres. The microsphere aggregates thus formed the particles with more separated aggregates which produced structures with small pores on the surface.

Figure 4.20 shows the electron micrographs of the surface of Sty-DVB copolymer of Sample L by variation of reaction times (240, 180 min). The reaction times increases, the surface of beads are increased to cause agglomeration of the microspheres. The same appearance was observed as those of Sample K.

4.6 Coefficients of partial correlation of parameter studies

Styrene-divinylbenzene copolymers were studied in the conversion of the individual monomers and the overall conversion were presented in Table 4.3-4.5 and 4.7-4.8. The results were used for coefficients of partial correlation that showed the relation between dependent parameters (styrene conversion, divinylbenzene conversion, ethylvinylbenzene conversion and overall conversion) with parameters as styrene, divinylbenzene, ethylvinylbenzene, initiator, toluene, poly(vinyl alcohol), temperature, agitation, time. The results were presented in Table 4.10.

Table 4.10 Coefficients of partial correlation of parameter

Parameter	Coefficients of partial correlation	Significance
Sty conversion – initiator	0.111	0.131
Sty conversion - agitation	0.030	0.383
Sty conversion – styrene	-0.003	0.490
Sty conversion - DVB	0.003	0.490
Sty conversion - EVB	0.002	0.491
Sty conversion - toluene	-0.101	0.154
Sty conversion – temperature	0.061	0.271
Sty conversion – time	0.718	0.000
DVB conversion – initiator	0.091	0.179
DVB conversion - agitation	0.026	0.397
DVB conversion – styrene	0.012	0.450
DVB conversion - DVB	-0.012	0.450
DVB conversion - EVB	-0.013	0.447
DVB conversion - toluene	-0.073	0.230
DVB conversion – temperature	0.056	0.287
DVB conversion – time	0.692	0.000

Table 4.10 Coefficients of partial correlation of parameter (continue)

Parameter	Coefficients of partial correlation	Significance
EVB conversion – initiator	0.062	0.530
EVB conversion - agitation	0.022	0.828
EVB conversion - EVB	-0.001	0.498
EVB conversion - toluene	-0.059	0.277
EVB conversion – temperature	0.036	0.358
EVB conversion – time	0.657	0.000
Overall conversion – initiator	0.217	0.013
Overall conversion - agitation	-0.033	0.370
Overall conversion – styrene	-0.083	0.201
Overall conversion - DVB	0.083	0.201
Overall conversion - EVB	0.087	0.190
Overall conversion - toluene	-0.173	0.039
Overall conversion – temperature	0.295	0.001
Overall conversion – time	0.762	0.000
Styrene – divinylbenzene	-1.0000	0.000
Styrene – ethylvinylbenzene	-0.9985	0.000
Divinylbenzene - ethylvinylbenzene	0.9985	0.000

สถาบันวิทยบริการ
จุฬาลงกรณ์มหาวิทยาลัย

A statistical test about the coefficients of partial correlation of parameter [25]

(H_0): $\rho_{y,xi} \leq 0$ VS (H_1): $\rho_{y,xi} > 0$; i =1,2,3,...

Rejection region: For a given value of $\alpha = 0.05$

Reject H_0 if sig. $< \alpha$

Significance of each parameter was compared with probability F. The values of significance were less than probability F that both of parameters had relation. The results showed that styrene conversion, divinylbenzene conversion, ethylvinylbenzene conversion and overall conversion were related with time. Overall conversion was related with the concentration of initiator, polymerization temperature and diluent concentration. Diluent was related minus value with overall conversion.

สถาบันวิทยบริการ
จุฬาลงกรณ์มหาวิทยาลัย

4.7 Glass transition temperatures

Glass transition temperatures and incremental changes in heat capacity at T_g were measured calorimetrically. In a DSC scan, the thermogram obtained therefore represents the glass transition temperature range. This is observed experimentally, as can be discerned in Figure 4.29 by comparing the thermograms obtained for Sample F (Sty 92.5%, DVB 7.5%, Tol 100%, 80°C, 240 rpm., BPO 0.5%) at 240, 180, 150, and 120 min. The T_g range is 107.15, 109.89, 109.57, and 108.33°C, respectively. In Figure 4.30 by comparing the thermograms obtained for Sample K (Sty 92.5%, DVB 7.5%, Tol 20%, 70°C, 240 rpm., BPO 0.5%) at 240, 180, 150, and 120 min. The T_g range is 109.73, 108.75, 106.89, and 107.64°C, respectively. The results indicate that T_g of styrene-divinylbenzene copolymers was about 106-110°C (polystyrene was 100°C [26]). Although T_g was influenced by copolymerization effects, the strong chemical similarity between styrene and divinylbenzene would suggest that the observed increase in T_g as the divinylbenzene content is increased is predominantly the result of crosslinking. The results indicate that the variation of reaction time is slightly different as reflected in the T_g of the copolymers due to the small amount of DVB crosslinked to styrene even though r_{DVB} is higher.

สถาบันวิทยบริการ
จุฬาลงกรณ์มหาวิทยาลัย

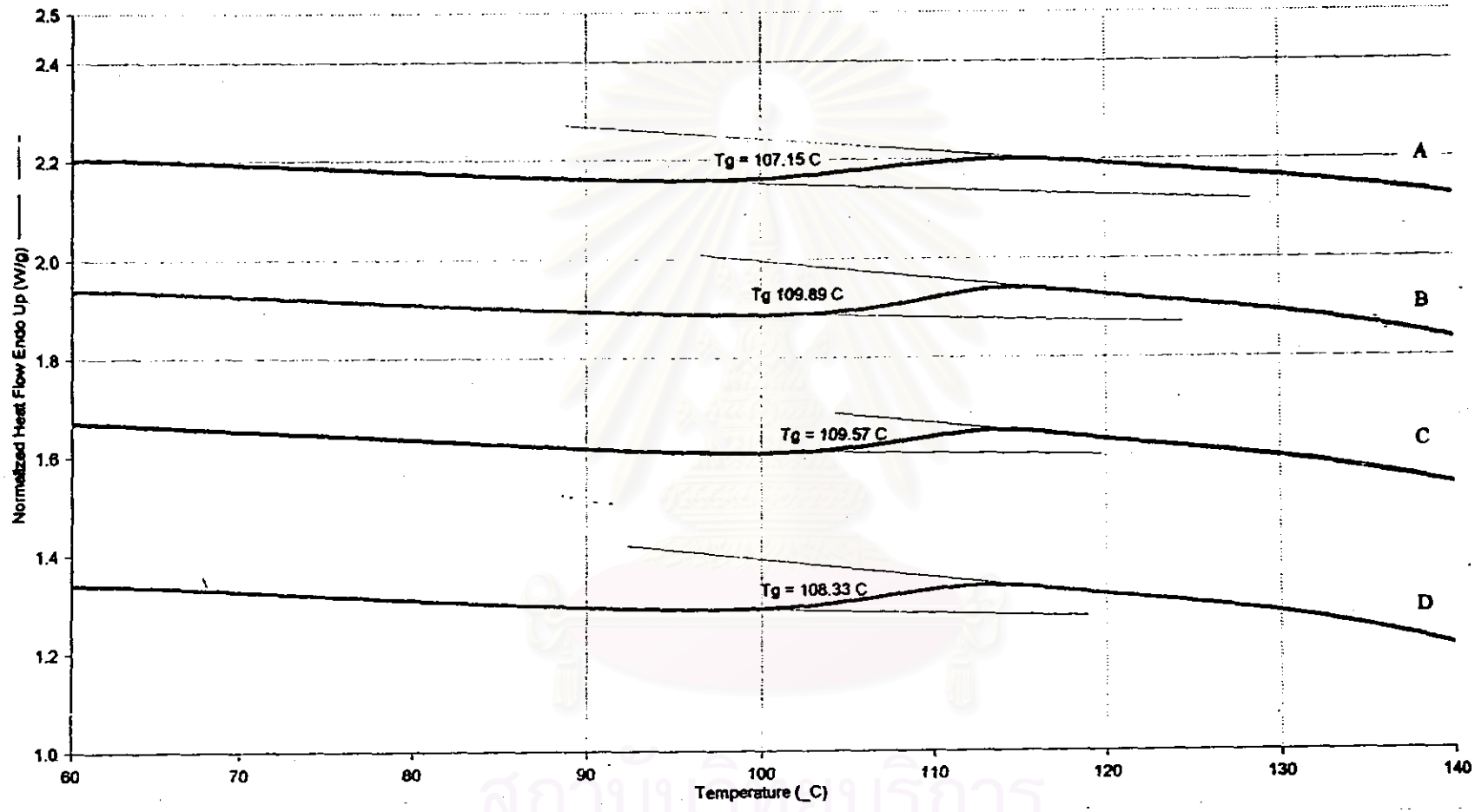

Figure 4.29 Typical DSC traces of the Sample F at 240, 180, 150, and 120 min. (The curves A, B, C, and D are for 240, 180, 150, and 120 min)

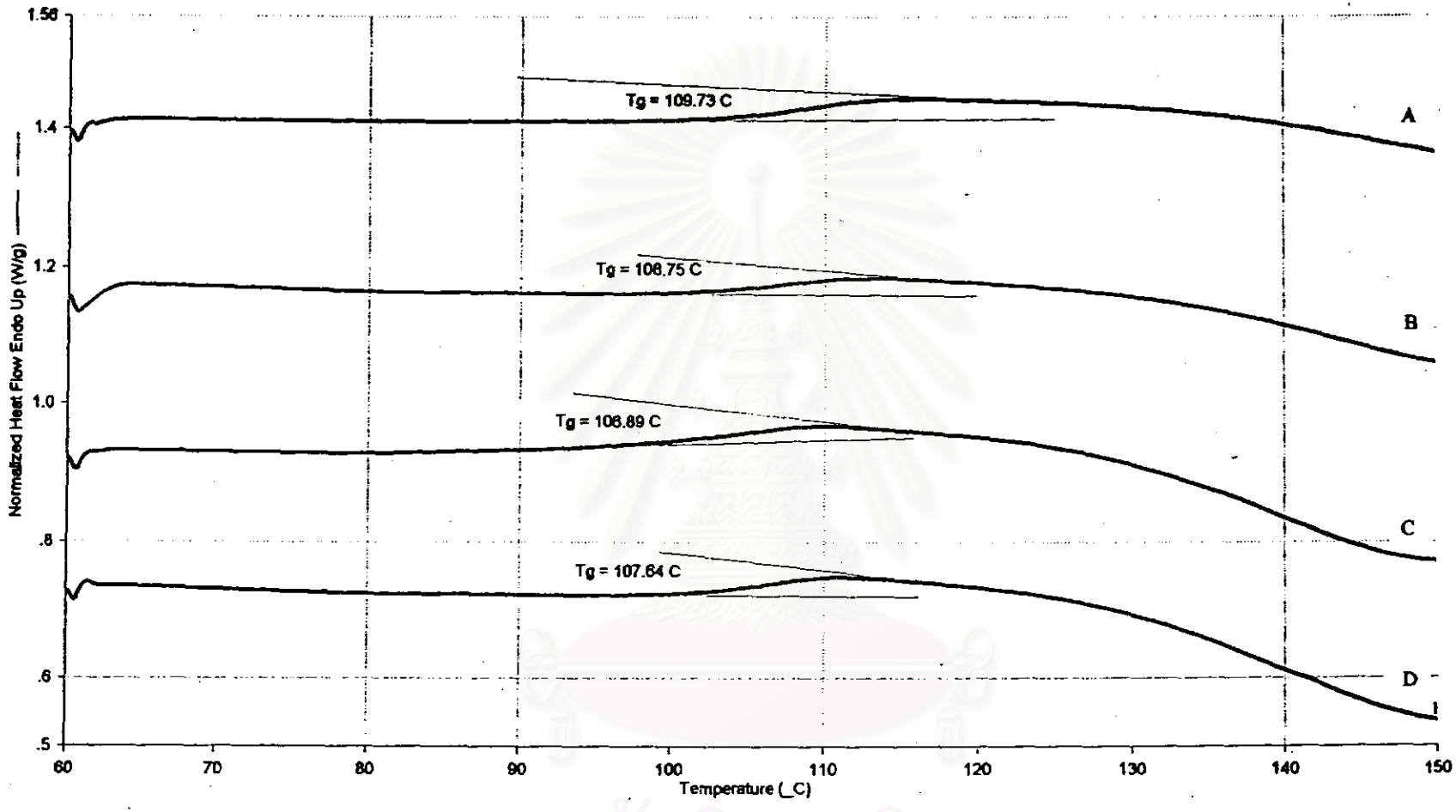

Figure 4.30 Typical DSC traces of the Sample K at 240, 180, 150, and 120 min. (The curves A, B, C, and D are for 240, 180, 150, and 120 min)

สถาบันวิทยบริการ
จุฬาลงกรณ์มหาวิทยาลัย

4.8 Infrared spectroscopy

The IR spectra of the styrene networks in KBr pellets were recorded on a Perkin-Elmer Ft-IR Spectrometer 1760. In order to characterize the copolymer beads and determine the crosslinking bond of divinylbenzene, the Sample B was analyzed by Infrared spectroscopy, compared with polystyrene, as shown in Figures 4.31 and 4.32. Figures 4.31 and 4.32 showed that the IR spectrum of both the polystyrene and the synthetic bead were rather similar, the assignments of the peaks are shown below [34].

Absorption frequency, cm^{-1}	Assignment
3080- 3010	: C-H stretching
2960- 2850	: C-H stretching of CH_3 and CH_2
2000- 1667	: benzenoid compounds
1660 - 1640	: C=C stretching (vinyl terminal)
770 - 730	: monosubstituted aromatic ring

To determine the crosslinking of divinylbenzene, the peak of para-disubstituted aromatic ring must be identified at 800-860 cm^{-1}, the peak of meta-disubstituted aromatic ring must be identified at 750-810 cm^{-1}. Therefore, the IR spectrum of both the beads and the polystyrene in this region can be discriminated from each other. Figure 4.31 cannot show the peaks of para-, meta-disubstituted groups due to that it is non-crosslinked but the peaks of para-, meta-disubstituted group are shown due to that it is crosslinked.

สถาบันวิทยบริการ
จุฬาลงกรณ์มหาวิทยาลัย

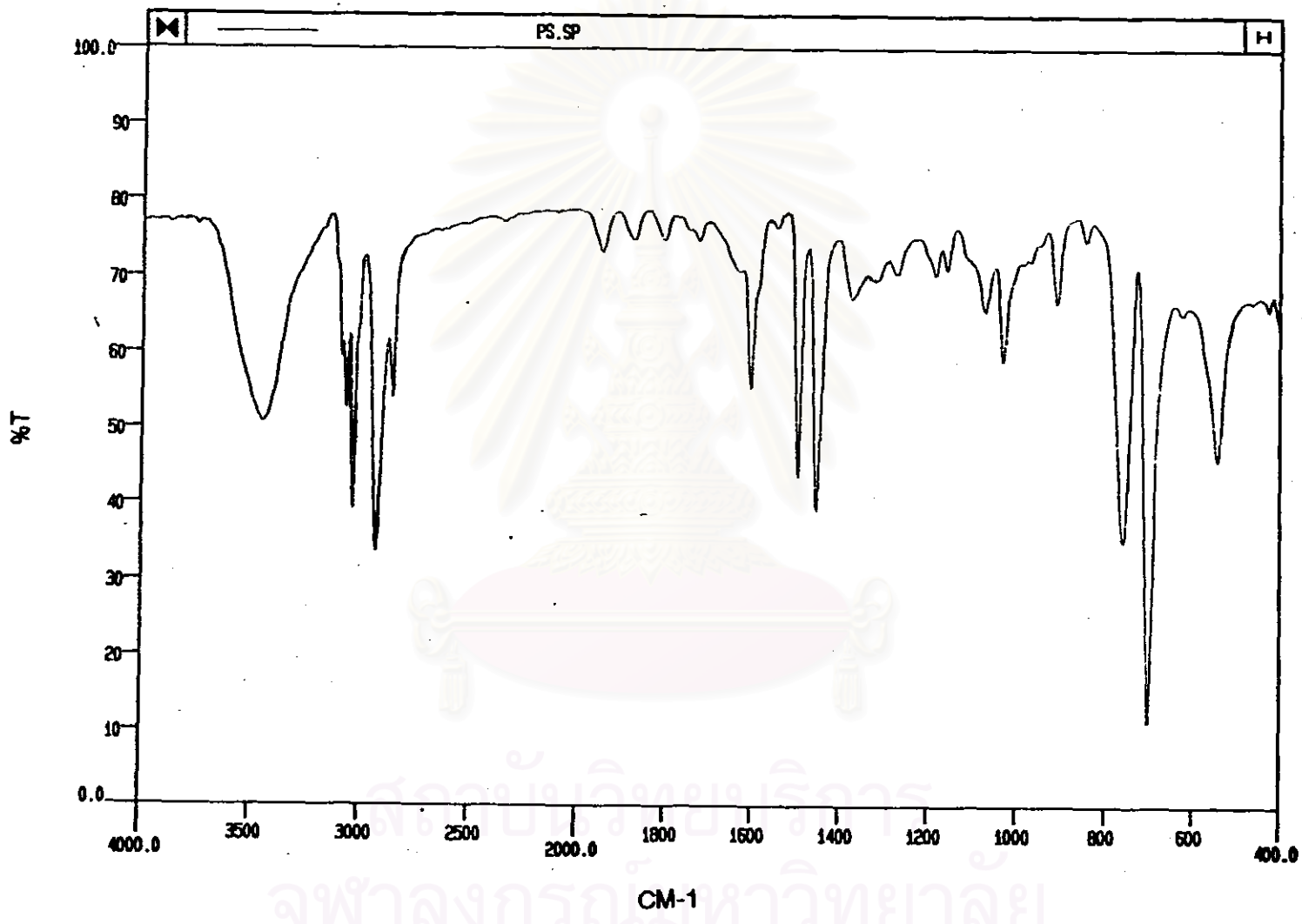

Figure 4.31 Infrared spectroscopy of polystyrene

สถาบันวิทยบริการ
จุฬาลงกรณ์มหาวิทยาลัย

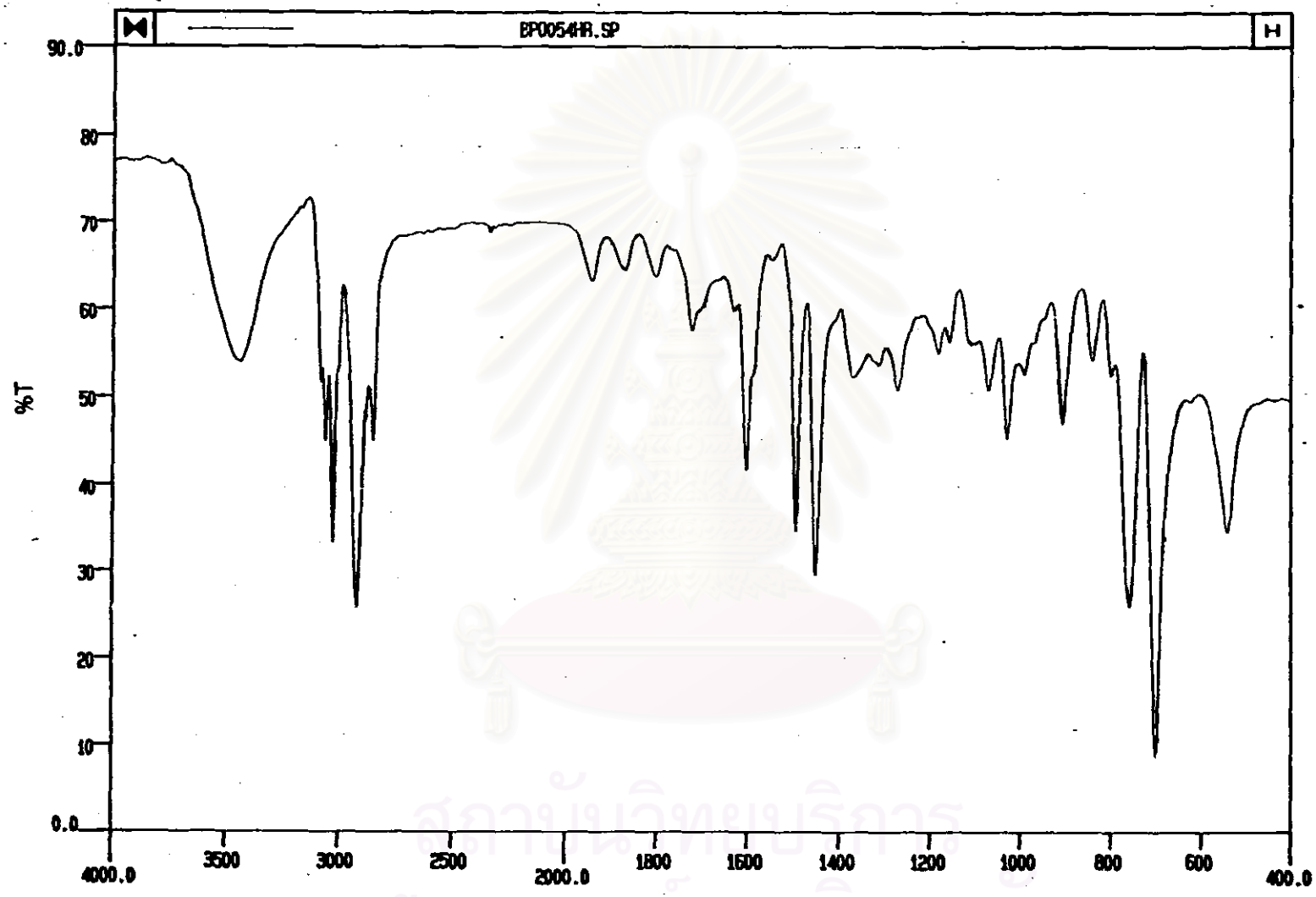

Figure 4.32 Infrared spectroscopy of styrene-divinylbenzene copolymer of Sample B at 240 min.

สถาบันวิทยบริการ
จุฬาลงกรณ์มหาวิทยาลัย

4.9 Production of styrene-divinylbenzene copolymers in a pilot scale

Table 4.11 Properties of styrene-divinylbenzene copolymers in a pilot scale[d]

Sample	Overall conversion, %	Swelling ratio	Particle sizes[c] (mm)
1[a]	43.4	7	< 0.42
2[b]	79.3	5	< 0.42

[a] Sty 92.5%, DVB 7.5%, BPO 0.5%, 240 rpm., 70°C, Tol 100%, PVA 0.09%, Monomer: H_2O, 1:7, 10 hours

[b] Sty 92.5%, DVB 7.5%, BPO 0.5%, 240 rpm., 80°C, Tol 100%, PVA 0.09%, Monomer: H_2O, 1:7, 10 hours

[c] Analysis of the particle size distribution by wire gauze of different mesh sizes that varying from 2 mm at the upper stack to 0.84, 0.59, and 0.42 mm at the lower stacks, respectively

[d] Characteristic of reactor is show in Appendix B.

Direct observations of styrene-divinylbenzene copolymer morphology by scanning electron microscopy of Samples 1, and 2 are shown in Figures 4.33 and 4.34, respectively.

Figure 4.35 shows the electron micrographs of the surface of styrene-divinylbenzene copolymer (Sample 2) by variation of reaction times (4, 6, and 8 hr.).

สถาบันวิทยบริการ
จุฬาลงกรณ์มหาวิทยาลัย

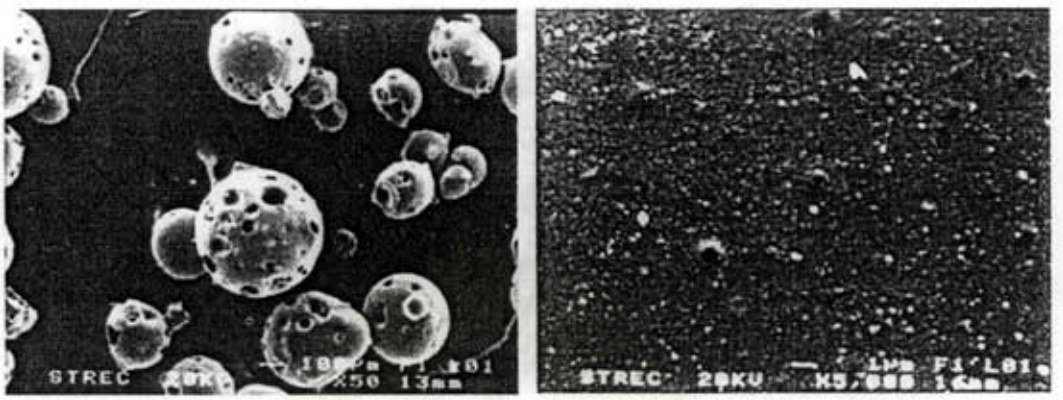

a) b)

Figure 4.33. Scanning Electron Micrographs of Sample 1: Sty 92.5%, DVB 7.5%, 70°C, BPO 0.5%, 240 rpm., Tol 100%, Monomer: H_2O 1:7 at 10 hr
a) x 50, b) x 5000

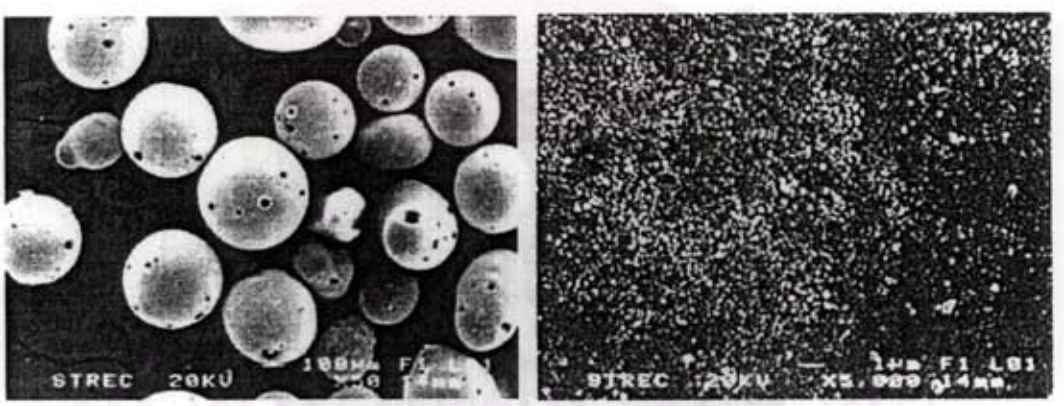

a) b)

Figure 4.34. Scanning Electron Micrographs of Sample 2: Sty 92.5%, DVB 7.5%, 80°C, BPO 0.5%, 240 rpm., Tol 100%, Monomer: H_2O 1:7 at 10 hr
a) x 50, b) x 5000

a)

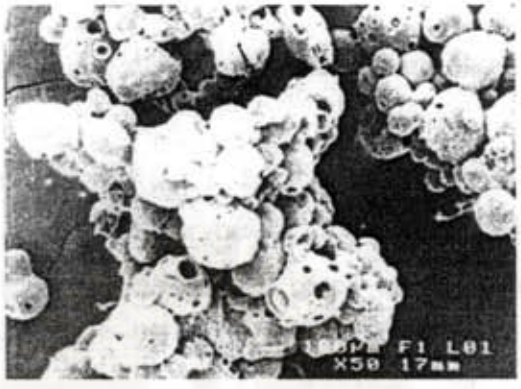

b)

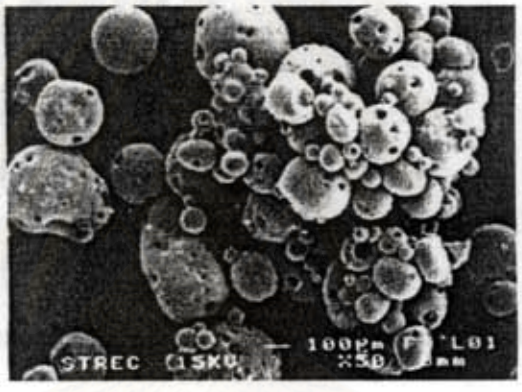

c)

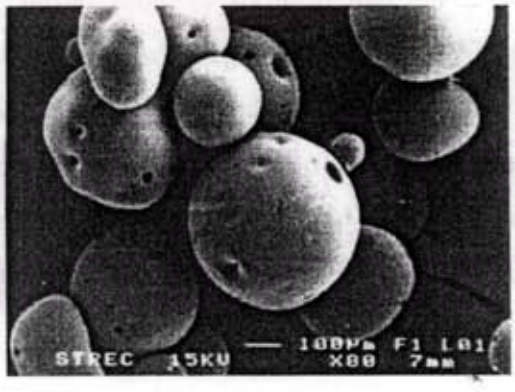

Figure 4.35. Scanning Electron Micrographs of Sample 2: Sty 92.5%, DVB 7.5%, 80°C, BPO 0.5%, 240 rpm., Tol 100%, Monomer: H_2O 1:7 at x 50
a) 4 hr, b) 6 hr, c) 8 hr

4.10 Absorption-desorption and diffusion coefficient in toluene of the beads

4.10.1 Absorption

The absorption of the imbiber beads in toluene which has a total solubility parameter of 18.6 $(MPa)^{1/2}$ was determined based on an increase in bead size upon swelling in good solvents.

Figure 4.36 shows the variation of bead volume with swelling time. The curves comprise three stages [15]:

I. An initial stage of the high sorption rate can be easily observed because the solubility parameter of toluene closes to that of the styrene-divinylbenzene copolymers and its chemical structure is similar to the styrene-divinylbenzene copolymers structure.

II. A second stage of the slow sorption rate is due to the sorption into the pore inclusive of pore structure and dimension.

III. A third stage of the plateau value because of the absorption saturation.

The increasing of bead volume with swelling time for the beads prepared by using toluene, as diluent. The initial stage of sorption was about 30 min, the bead volume increased rapidly since the network began to expand by absorbing the surrounding solvent. Finally, the swollen bead reached a stationary state in equilibrium with the surrounding solvent within 60 min. The diffusion coefficient (see Appendix C) of Sample B was 0.085 and 0.083 mm^2/min or 1.41×10^{-5} and 1.39×10^{-5} cm^2/sec, respectively and Sample L was 0.089 and 0.087 mm^2/min or $1.49 \times 10^{-5}$and 1.45×10^{-5} cm^2/sec, respectively.

4.10.2 Desorption

When a swollen bead was placed on the filter paper, the solvent diffused from the bead and got in to the filter paper. It may be possible to that the interaction between

solvent and the substrate is higher than the interaction between the solvent and the polymer network.

Figure 4.37 shows the variation of swollen bead volume with time. These curves can be divided into three stages [15]:

I. An initial stage of the high desorption rate. Since the cellulosic substrate is high by absorptive.

II. A second stage of slow desorption rate.

III. A third stage of no solvent loss (plateau) or a very low, undetectable desorption rate due to the relatively high vapor pressure of toluene (3.8 kPa).

For the decreasing of the swollen bead volume with time for the beads prepared by using toluene, as diluent, the initial stage of desorption was about 10 min, and then the swollen bead lost all solvent within 40 min after the start of desorption process.

สถาบันวิทยบริการ
จุฬาลงกรณ์มหาวิทยาลัย

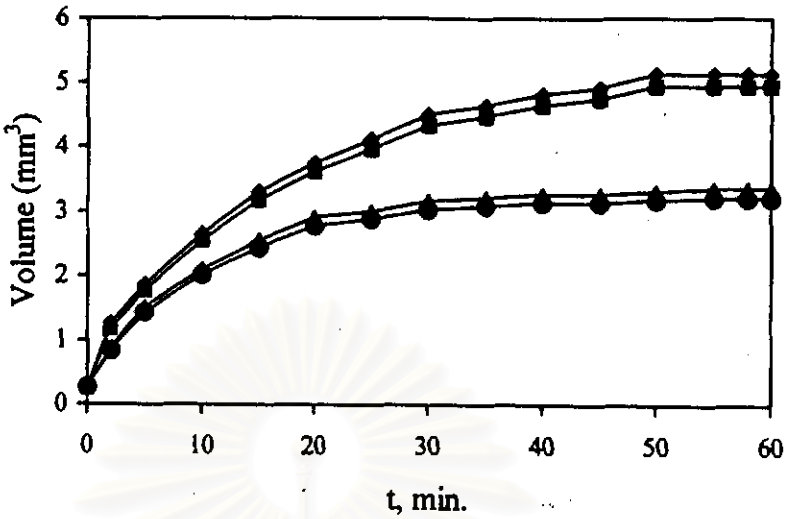

Figure 4.36 Variation of bead volume with time: (The curves ♦ ♦ ♦, ■■■, ▲▲▲, and ●●● are for absorption of Sample B 1, absorption of Sample B 2, absorption of Sample L 1, absorption of Sample L 2)

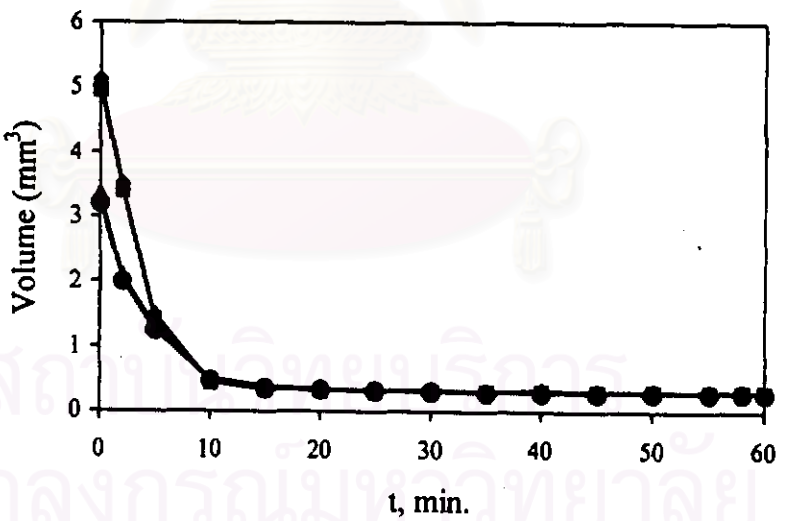

Figure 4.37 Variation of bead volume with desorption time: (The curves ♦ ♦ ♦, ■■■, ▲▲▲, and ●●● are for desorption of Sample B 1, desorption of Sample B 2, desorption of Sample L 1, desorption of Sample L 2)

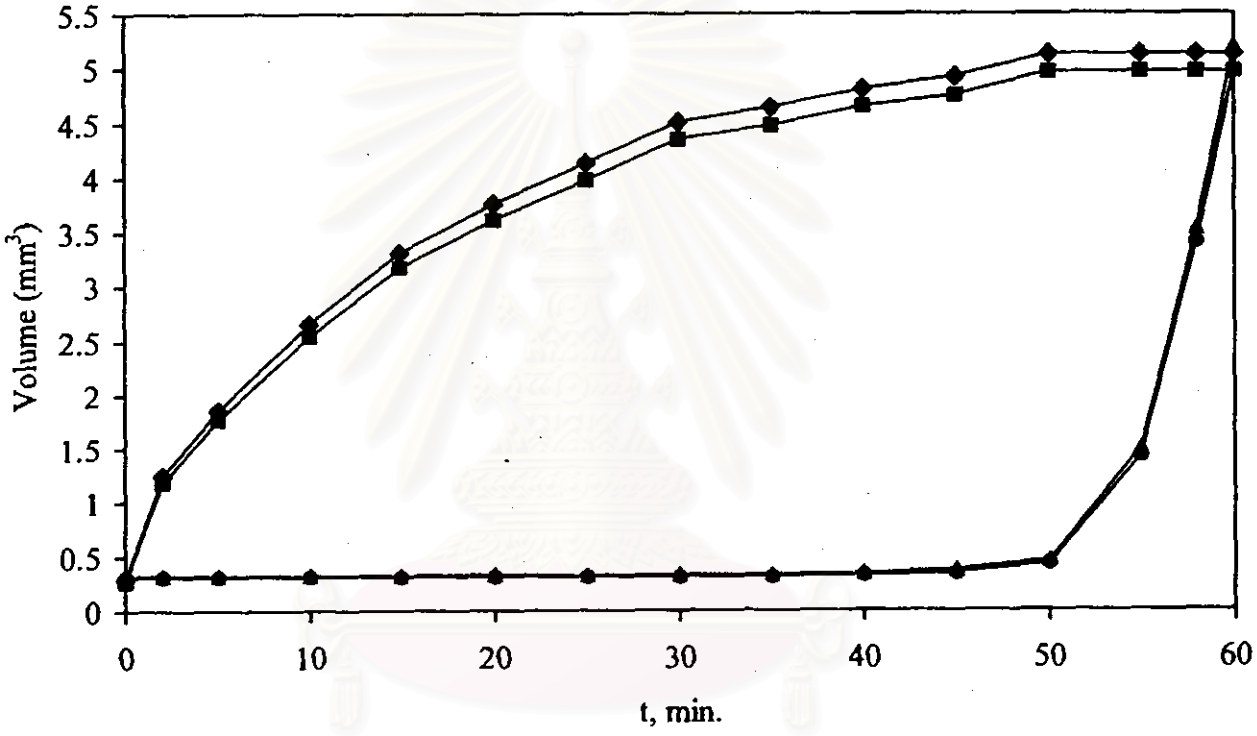

Figure 4.38 Variation of bead volume with time: Sample B at 240 min.(The curves ♦♦♦, ■■■, ▲▲▲, and ●●● are for absorption 1, absorption 2, desorption 1, desorption 2; when Sty 92.5%, DVB 7.5%, BPO 0.5%, 240 rpm., Tol 100%, PVA 0.09%, Monomer: H_2O, 1:7)

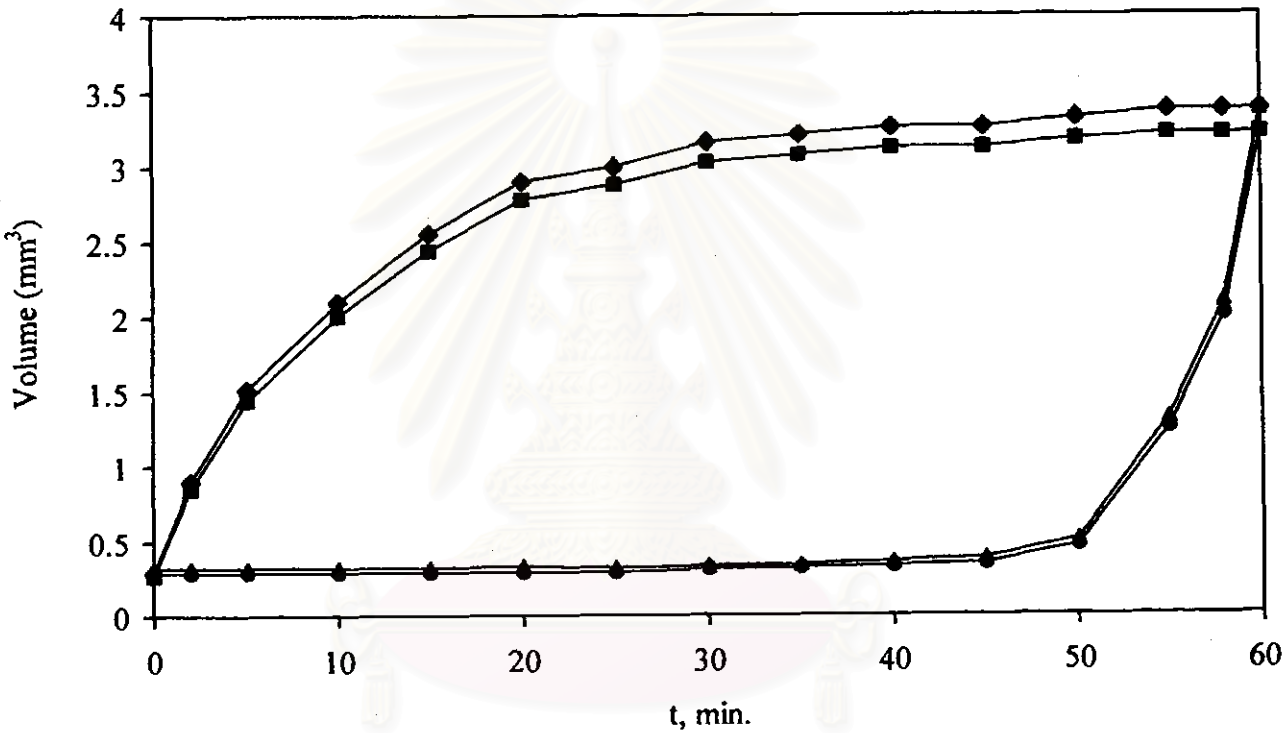

Figure 4.39 Variation of bead volume with time: Sample L at 240 min.(The curves ♦♦♦, ■■■, ▲▲▲, and ●●● are for absorption 1, absorption 2, desorption 1, desorption 2; when Sty 92.5%, DVB 7.5%, BPO 0.5%, 240 rpm., Tol 60%, PVA 0.09%, Monomer: H_2O, 1:7)

4.11 Rate equation

4.11.1 Integral Method of Analysis of Data

The integral method of analysis always puts a particular rate equation to the test by integrating. In a constant volume system, the examination for fitting simple reaction types corresponding to elementary reactions.

The concentration of Samples A, B, C, D, G and H were averaged for searching a kinetic equation that the data are well fitted.

Table 4.12 The concentration of each components at the polymerization intervals of 30, 60, 90, 120, 150, 180 and 240 min at polymerization temperature 70°C

Time (min.)	Sty (C_A) (mol/l)	DVB (C_B) (mol/l)	EVB (C_D) (mol/l)
0	3.9379	0.1585	0.0789
30	0.7624	0.0235	0.0087
60	0.6667	0.0201	0.0078
90	0.5149	0.0150	0.0060
120	0.4037	0.0113	0.0045
150	0.3014	0.0086	0.0035
180	0.2313	0.0058	0.0026
240	0.1831	0.0043	0.0020

4.11.1.1 Irreversible Unimolecular-type First-order Reaction, one considers the following reaction [36]

$$A \rightarrow products \tag{4.4}$$

with the corresponding rate equation

$$-r_A = -\frac{dC_A}{dt} = kC_A \tag{4.5}$$

the integration form is

$$-\ln\frac{C_A}{C_{A0}} = kt \tag{4.6}$$

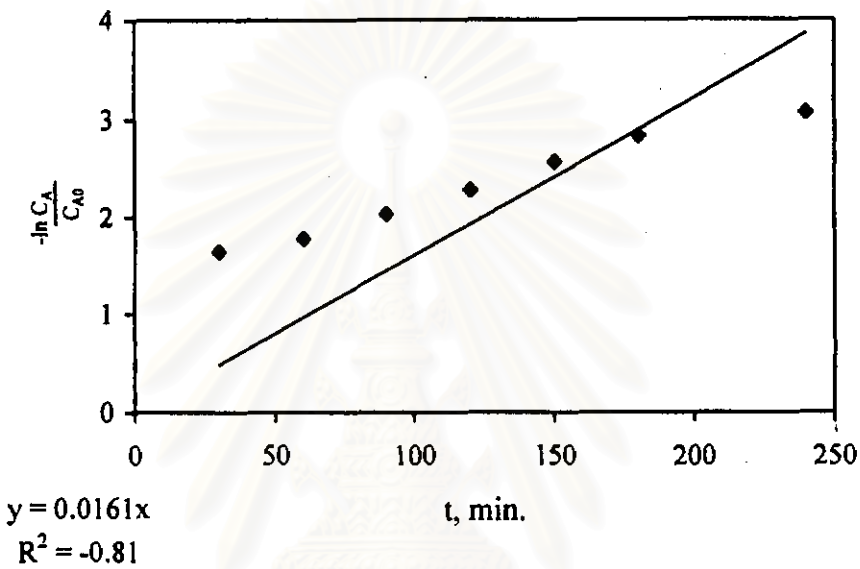

Figure 4.40 Test for the first-order reaction of equation 4.6

The fit is unsatisfactory, then this rate equation and its mechanism are rejected. Other rate equation is tried.

4.11.1.2 Irreversible Bimolecular-type Second-order Reaction, one considers the following reaction

$$2A \rightarrow products \tag{4.7}$$

with the corresponding rate equation

$$-r_A = -\frac{dC_A}{dt} = kC_A^2 \tag{4.8}$$

the integration form is

$$\frac{1}{C_A} - \frac{1}{C_{A0}} = kt \tag{4.9}$$

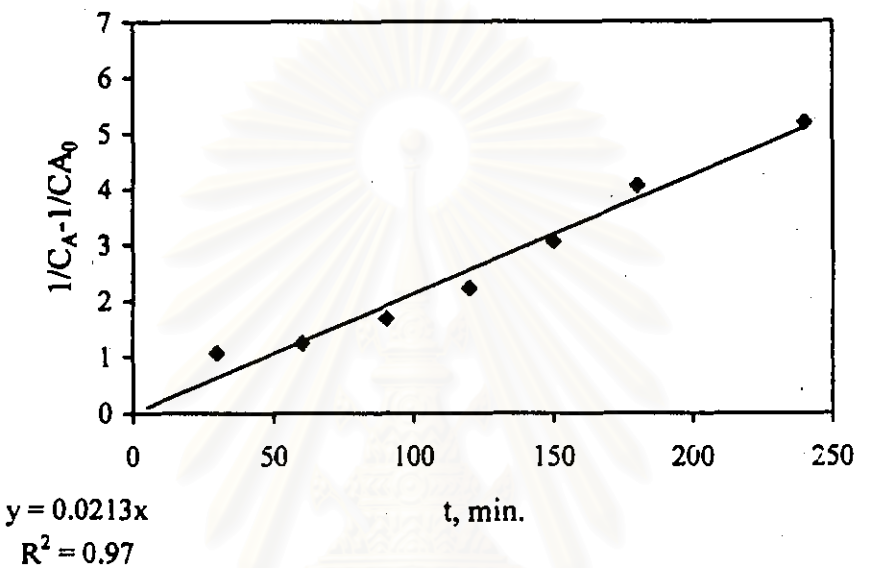

Figure 4.41 Test for the second-order reaction of equation 4.9

These data fall on a reasonably straight line passing through the origin, (R^2=0.97) the equation of this reaction is the second-order kinetic and the slope or k is 0.0213. Therefore, the rate of the second order reaction is

$$-r_A = 0.0213\ C_A^2 \tag{4.10}$$

where C_A is concentration of styrene

4.11.1.3 Irreversible Trimolecular-type Third-order Reaction, one considers the following reaction

$$A + B \rightarrow products \tag{4.11}$$

with the corresponding rate equation

$$-r_A = -\frac{dC_A}{dt} = kC_A C_B^2 \tag{4.12}$$

the integration form is

$$\frac{(C_{A0} - C_{B0})(C_{B0} - C_B)}{C_{B0}C_B} + \ln\frac{C_{A0}C_B}{C_{B0}C_A} = (C_{A0} - C_{B0})^2 kt \tag{4.13}$$

for $M \neq 1$, where $M = C_{B0}/C_{A0}$

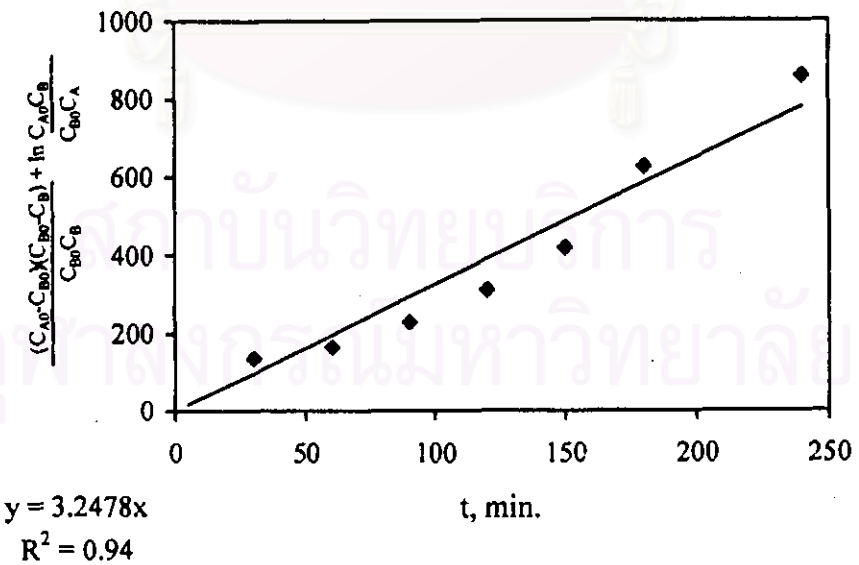

Figure 4.42 Test for the third-order reaction of equation 4.13

These data fall on a reasonably straight line passing through the origin, (R^2=0.97) the equation of this reaction is the third-order kinetic and the slope is 3.2478.

$$(C_{A0} - C_{B0})^2 k = 3.2478$$

$$k = \frac{3.2478}{(3.9379 - 0.1585)^2} = 0.2274$$

therefore, the rate of the third order reaction is

$$-r_A = 0.2274\ C_A\ C_B^2 \qquad (4.14)$$

where C_A is concentration of styrene

C_B is concentration of divinylbenzene

Therefore, an elementary reaction was well correlated by the following rate equation:

$$-r_A = 0.0213\ C_A^2$$

4.11.1.4 Temperature-dependent term of rate constant

The concentrations of Samples E and F were plotted by second-order reactions (Eq 4.9).

Table 4.13 Monomer concentration dependence on reaction time at polymerization temperature 60°C and 80°C for styrene

Time (min.)	Sty (C_A) (mol/l) 60°C	Sty (C_A) (mol/l) 80°C
0	3.9379	3.9379
30	0.6983	0.5163
60	0.6666	0.4803
90	0.6513	0.3628
120	0.6469	0.2452
150	0.6075	0.2271
180	0.4883	0.1875
240	0.2079	0.0991

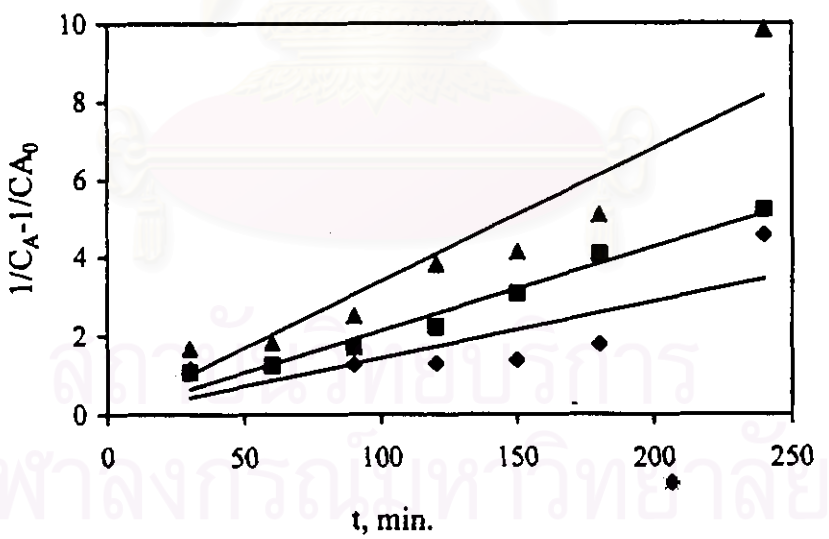

Figure 4.43 Test for the second-order reactions of equation 4.9 of the temperature; (The curves ♦♦♦, ■■■, and ▲▲▲ are for temperature 60, 70, and 80°C; when Sty 92.5%, DVB 7.5%, BPO 0.5%, 240 rpm., Tol 100%, Monomer: H_2O, 1:7; are used).

Table 4.14 Rate constants of second-order reaction with temperature

Temperature (°C)	Rate equation	R^2	k (l/mole.min)
60	y = 0.0144x	0.63	0.0144
70	y = 0.0213x	0.97	0.0213
80	y = 0.0340x	0.88	0.0340

The reaction has a higher rate constant at high temperatures according to Arrhenius equation.

4.11.1.5 Activation energy and temperature dependency [37]

From Arrhenius' law

$$k(T) = k_0 e^{-E/RT} \tag{4.15}$$

after taking the natural logarithm of Eq. (4.15)

$$\ln k = \ln k_0 - \frac{E}{R}\left(\frac{1}{T}\right) \tag{4.16}$$

By converting Eq. (4.16) to log base 10

$$\log k = \log k_0 - \frac{E}{2.3R}\left(\frac{1}{T}\right) \tag{4.17}$$

We can use the semilog scale to determine E quite readily based on the data in Table 4.15.

Table 4.15 Data of the rate constant with temperature

T (°C)	T (K)	k	1/T (K^{-1})	log k
60	333	0.0144	0.003003	-1.8416
70	343	0.0252	0.002915	-1.6716
80	353	0.0340	0.002833	-1.4685

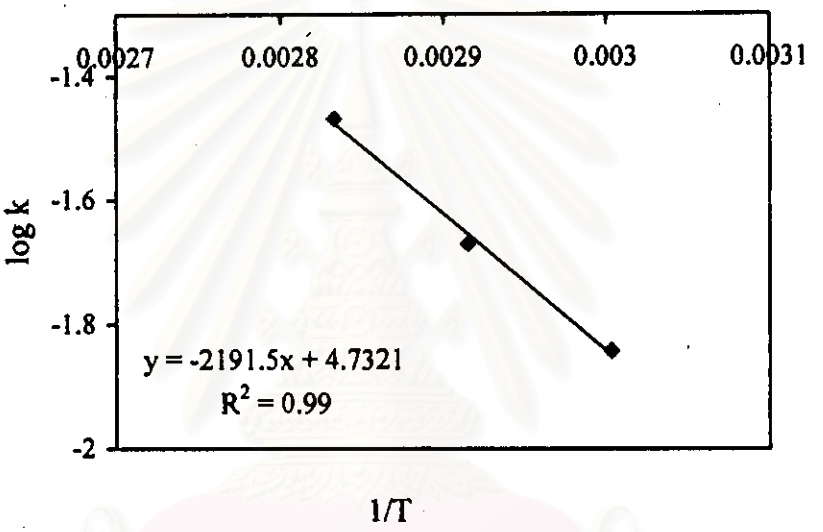

Figure 4.44 Temperature dependency of the rate constant

From Equation (4.17)

$$\log k = 4.7321 - 2191.5\left(\frac{1}{T}\right) \tag{4.18}$$

$$\frac{E}{2.3R} = 2{,}191.5 \tag{4.19}$$

$$E = 2{,}191.5 \times 2.3R$$
$$= 2{,}191.5 \times 2.3 \times 1.987$$
$$= 10{,}015 \ \ Cal./mol$$

4.11.2 Differential Method of Analysis of Data

The differential method of analysis deals directly with the differential rate equation as follows. We consider a reaction carried out in a constant volume and the concentration recorded as a function of time as shown in Table 4.12.

$$-\frac{dC_A}{dt} = kC_A^{\alpha} \tag{4.20}$$

After taking the natural logarithm of both sides of Eq (4.20)

$$\ln(-\frac{dC_A}{dt}) = \ln k + \alpha \ln C_A \tag{4.21}$$

The reaction order can now be found from a plot of $\ln(-dC_A/dt)$ as a function of $\ln C_A$ (the data are shown in APPENDIX H),

For Styrene,

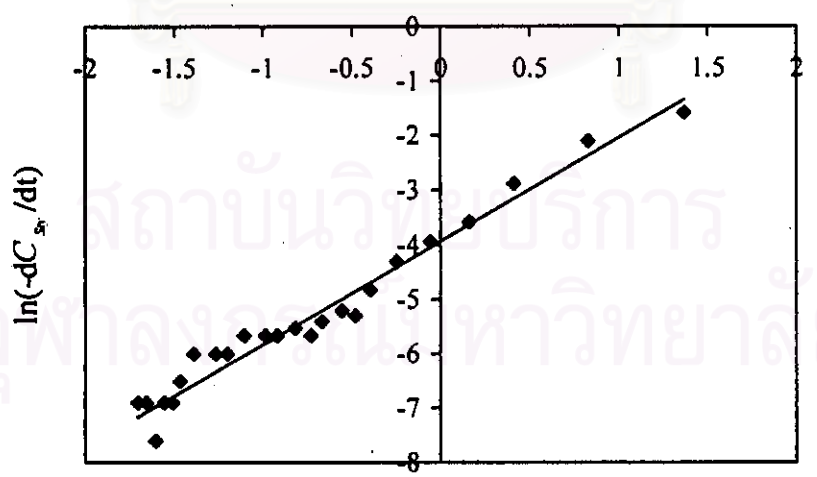

Figure 4.45 Differential method for determining the reaction order of styrene

For Divinylbenzene,

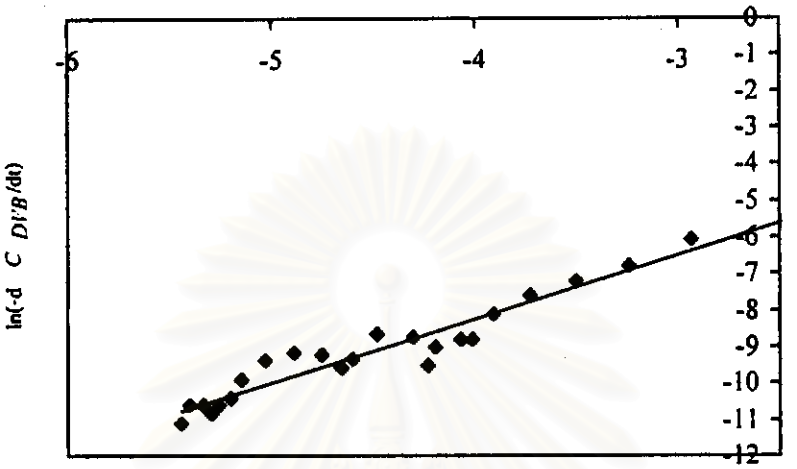

Figure 4.46 Differential method for determining the reaction order of divinylbenzene

For Ethylvinylbenzene,

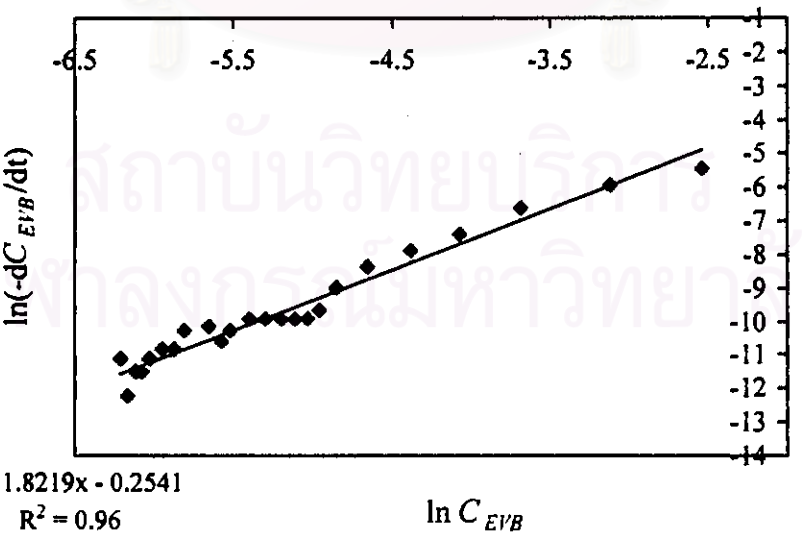

Figure 4.47 Differential method for determining the reaction order of ethyl vinylbenzene

Using the line through the data points in Figures 4.45- 4.47:

For Styrene,

α = slope = 1.9 and k = 0.0197

For Divinylbenzene,

α = slope = 1.8 and k = 0.2908

For Ethylvinylbenzene,

α = slope = 1.8 and k = 0.7756

The rate equations (rate of calculation) for reactant are

For Styrene, $-r_{Sty} = 0.0197\, C_{Sty}^{1.9}$ R^2= 0.96

For Divinylbenzene, $-r_{DVB} = 0.2908\, C_{DVB}^{1.8}$ R^2= 0.95

For Ethylvinylbenzene, $-r_{EVB} = 0.7756\, C_{EVB}^{1.8}$ R^2= 0.96

We consider a reaction of each sample(A-D, G, H) carried out in a constant volume and the concentration recorded as a function of time. We can calculate rate of experiment of each sample in the following,

The rate equations (rate of experiment) for Sample A are

For Styrene, $-r_{Sty} = 0.0086\, C_{Sty}^{1.8}$ R^2= 0.77

For Divinylbenzene, $-r_{DVB} = 0.1368\, C_{DVB}^{1.8}$ R^2= 0.80

For Ethylvinylbenzene, $-r_{EVB} = 0.5895\, C_{EVB}^{1.9}$ R^2= 0.86

The rate equations (rate of experiment) for Sample B are

For Styrene, $-r_{Sty} = 0.0247\, C_{Sty}^{2.1}$ $R^2 = 0.91$

For Divinylbenzene, $-r_{DVB} = 0.3556\, C_{DVB}^{1.8}$ $R^2 = 0.83$

For Ethylvinylbenzene, $-r_{EVB} = 0.6327\, C_{EVB}^{1.8}$ $R^2 = 0.92$

The rate equations (rate of experiment) for Sample C are

For Styrene, $-r_{Sty} = 0.0288\, C_{Sty}^{2.5}$ $R^2 = 0.84$

For Divinylbenzene, $-r_{DVB} = 0.5860\, C_{DVB}^{1.9}$ $R^2 = 0.91$

For Ethylvinylbenzene, $-r_{EVB} = 1.3468\, C_{EVB}^{1.9}$ $R^2 = 0.89$

The rate equations (rate of experiment) for Sample D are

For Styrene, $-r_{Sty} = 0.0313\, C_{Sty}^{1.6}$ $R^2 = 0.95$

For Divinylbenzene, $-r_{DVB} = 0.0667\, C_{DVB}^{1.2}$ $R^2 = 0.88$

For Ethylvinylbenzene, $-r_{EVB} = 0.3567\, C_{EVB}^{1.5}$ $R^2 = 0.95$

สถาบันวิทยบริการ
จุฬาลงกรณ์มหาวิทยาลัย

The rate equations (rate of experiment) for Sample G are

For Styrene, $-r_{Sty} = 0.0142\, C_{Sty}^{2.2}$ $R^2 = 0.96$

For Divinylbenzene, $-r_{DVB} = 0.0950\, C_{DVB}^{1.4}$ $R^2 = 0.94$

For Ethylvinylbenzene, $-r_{EVB} = 0.1718\, C_{EVB}^{1.5}$ $R^2 = 0.91$

The rate equations (rate of experiment) for Sample H are

For Styrene, $-r_{Sty} = 0.0207\, C_{Sty}^{2.3}$ $R^2 = 0.88$

For Divinylbenzene, $-r_{DVB} = 1.4055\, C_{DVB}^{2.2}$ $R^2 = 0.84$

For Ethylvinylbenzene, $-r_{EVB} = 1.9658\, C_{EVB}^{2.0}$ $R^2 = 0.95$

The rate of calculation was compared with the rate of experiment when concentration of each monomer was placed in equation that the results as shown in Figure 4.48. The rate of experiment was close to the rate of calculation that the deviation was sample A as initiator concentration 0.1%. The complete simple rate equation of reaction was

$$-r\, \alpha\, C_{Sty}^{1.9}\ C_{DVB}^{1.8}\ C_{EVB}^{1.8} \qquad (4.22)$$

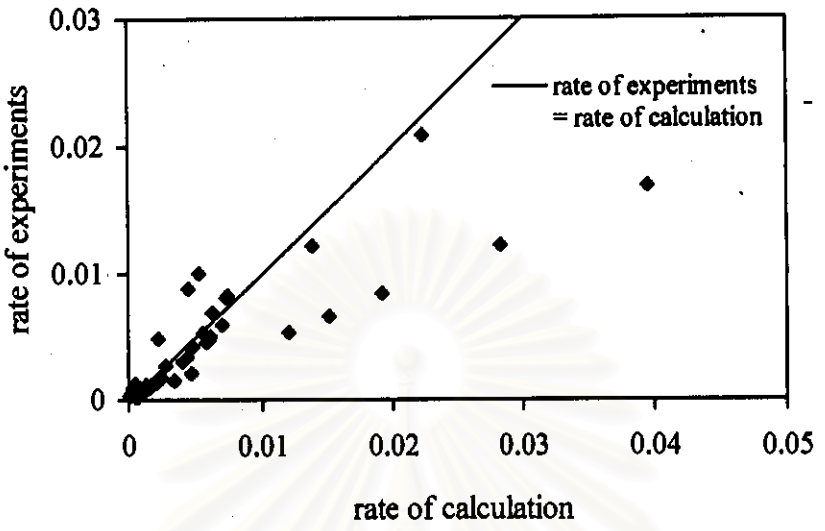

Figure 4.48 Test rate of experiment for compare with rate of calculation

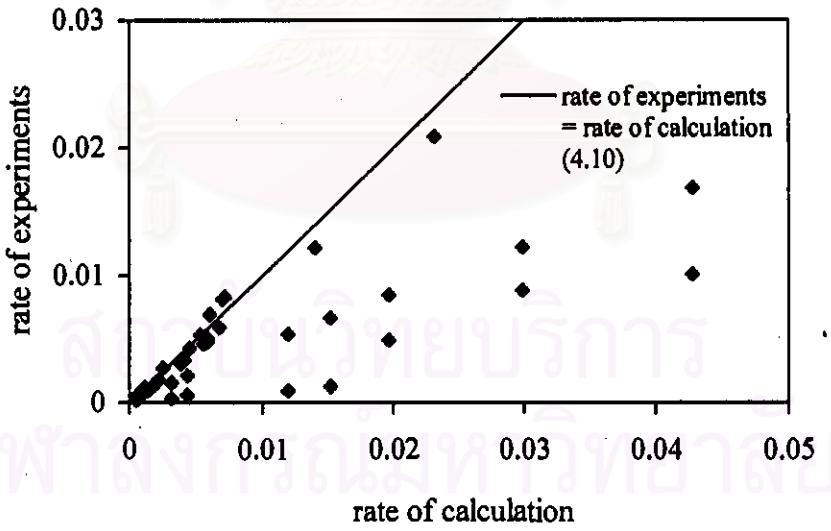

Figure 4.49 Test rate of experiment for compare with rate of calculation in equation (4.10)

From the rate of calculation in equation (4.10) was compared with the rate of experiment. Concentration of each monomer was placed in equation that the results as shown in Figure 4.49. The deviations were sample A and sample D as initiator concentration 0.1% and 2.0%, respectively. The rate of calculation by differential method was more accurate than the rate of calculation by integral method. Thus, the complete simple rate equation of reaction was

$$-r \alpha C_{Sty}^{1.9} \; C_{DVB}^{1.8} \; C_{EVB}^{1.8}$$

สถาบันวิทยบริการ
จุฬาลงกรณ์มหาวิทยาลัย